

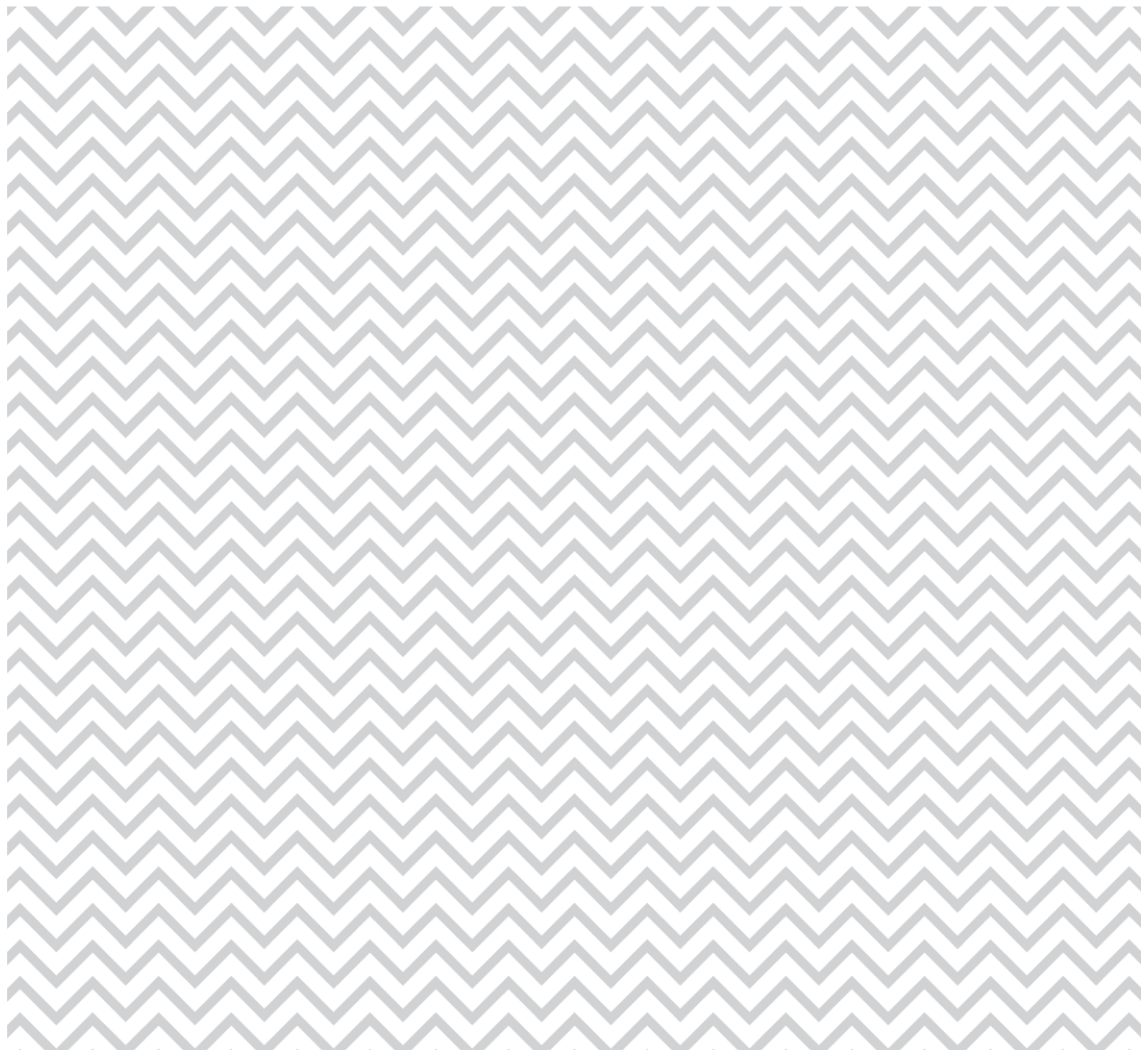


Norwegian  
Meteorological  
Institute

**MET report** no. 32/2013  
Oceanography

# BaSIC validation - addendum 1

Nils Melsom Kristensen, Arne Melsom, Yvonne Gusdal, Lars Petter Røed, Bjørn Ådlansvik (IMR), Jon Albretsen (IMR)







<b>Title:</b> BaSIC validation - addendum 1	<b>Date</b> 2013-12-13
<b>Section:</b> Research and Development – Dept. for Ocean and Ice	<b>Report no.</b> no. 32/2013
<b>Author(s):</b> Nils Melsom Kristensen, Arne Melsom, Yvonne Gusdal, Lars Petter Røed, Bjørn Ådlansvik (IMR), Jon Albretsen (IMR)	<b>Classification</b> <input type="radio"/> Free <input checked="" type="radio"/> Restricted
<b>Client(s):</b> Statoil	<b>Client's reference</b> 4502465983
<b>Abstract</b> This report is an addendum to MET report no. 12/2013. We present and explain the most recent results from the trial hindcasts phase of the project BaSIC, and a thorough validation of the results. This additional trial hindcast differs from the earlier ones in two main respects: First, we no longer use results from the SVIM4 model, and second, we have switched the vertical mixing scheme. The SVIM4 results are replaced by a run with the BaSIC20 model (20 km mesh size) using the UK Met Office model FOAM reanalysis on the open boundaries and ERA reanalysis as atmospheric forcing. BaSIC20 covers the entire Arctic region from approximately 50N in the Atlantic and just through the Bering Strait. Inside the BaSIC20 model, we have nested the BaSIC4 model (4 km mesh size) which covers the same area as SVIM4 (Nordic Seas). The BaSIC20 and BaSIC4 models have been run for 17 and 3 years, respectively, and the period 2000 – 2001 has been validated with regards to hydrography, sea-ice and currents. We are very happy to report that this new configurations show very promising results compared to the results presented in MET report 12/2013.	
<b>Keywords</b> ROMS, Ocean modeling, Barents Sea, Hindcast, Validation, Currents, Sea-Ice, Hydrography	

---

Disiplinary signature

---

Responsible signature



## Abstract

This report is an addendum to MET report no. 12/2013. We present and explain the most recent results from the trial hindcasts phase of the project BaSIC, and a thorough validation of the results. This additional trial hindcast differs from the earlier ones in two main respects: First, we no longer use results from the SVIM4 model, and second, we have switched the vertical mixing scheme. The SVIM4 results are replaced by a run with the BaSIC20 model (20 km mesh size) using the UK Met Office model FOAM reanalysis on the open boundaries and ERA reanalysis as atmospheric forcing. BaSIC20 covers the entire Arctic region from approximately 50N in the Atlantic and just through the Bering Strait. Inside the BaSIC20 model, we have nested the BaSIC4 model (4 km mesh size) which covers the same area as SVIM4 (Nordic Seas). The BaSIC20 and BaSIC4 models have been run for 17 and 3 years, respectively, and the period 2000 – 2001 has been validated with regards to hydrography, sea-ice and currents. We are very happy to report that this new configurations show very promising results compared to the results presented in MET report 12/2013.



# Table of contents

<b>1</b>	<b>Introduction</b>	<b>15</b>
<b>2</b>	<b>BaSIC20 model</b>	<b>17</b>
2.1	Model results	17
2.1.1	Currents	17
2.1.2	Sea ice	18
2.2	Validation	21
2.2.1	Currents	21
2.2.2	Volume fluxes	27
2.2.3	Temperature and salinity	29
2.2.4	Sea ice	32
<b>3</b>	<b>BaSIC4 model</b>	<b>34</b>
3.1	Model results	34
3.1.1	Currents	34
3.1.2	Sea ice	35
3.2	Validation	37
3.2.1	Currents	37
3.2.2	Temperature and salinity	41
3.2.3	Sea ice	47
<b>4</b>	<b>Comparison of current speed for different model resolution</b>	<b>48</b>
<b>5</b>	<b>Conclusions and recommendations</b>	<b>53</b>
5.1	Conclusions	53
5.2	Recommendations	53
	<b>Acknowledgements</b>	<b>55</b>
	<b>References</b>	<b>56</b>



## List of figures

Figure 1: The new grid configuration used in the final trial hindcast	15
Figure 2: Averaged surface currents over the simulation period 1993 - 2010.	17
Figure 3: Maximum current speed over the simulation period 1993 - 2010.	18
Figure 4: Maximum ice concentration for the model domain over the period 1995 - 2010. Note that this maximum concentration for each grid point, this did not necessarily happen at the same time.	18
Figure 5: Same as Figure 4, but minimum extent.	19
Figure 6: Same as Figure 4, but based on OSISAF satellite observations.	19
Figure 7: Same as Figure 6, but for minimum extent.	20
Figure 8: Position of stations for current measurements.	21
Figure 9: Frequency diagrams of current speed (in cm/s) over the years 2000 - 2011 in the Fugløya - Bjørnøya section at each station (CM1 - CM5). The left column shows results at 50m depth, and the right column shows results for the bottom depths. Red lines are observations and blue lines are the BaSIC20 model results.	22
Figure 10: Frequency diagrams of current direction over the years 2000 - 2011 in the Fugløya - Bjørnøya section at each station (CM1 - CM5). The left column shows results at 50m depth, and the right column shows results for the bottom depths. Red lines are observations and blue lines are the BaSIC20 model results.	23
Figure 11: Frequency diagrams of current direction over the years 2000 - 2011 in the Fugløya - Bjørnøya section at each station (CM1 - CM5). The left column shows results at 50m depth, and the right column shows results for the bottom depths. Red lines are observations and blue lines are the BaSIC20 model results.	24
Figure 12: Distribution of current direction together with current speed for the year 2000 -2011 in the Fugløya-Bjørnøya section at 50m depth at station CM1 through CM5. The first column show results for the current meter data and the second column the BaSIC20 model currents.	25
Figure 13: Same as Figure 12, but for the bottom.	26
Figure 14: Overview of the mean volume fluxes in Sverdrup trough different sections. Values in blue are from the BaSIC20 simulation and the red values from the SVIM4 simulation. Red values with an "A" represents Atlantic Water only.	27
Figure 15: Barents Sea Opening (BSO) volume flux, one year moving average.	28
Figure 16: Qq-plot of Atlantic volume flux in BSO as monthly values.	28

Figure 17: Seasonal variability of BSO volume flux.	29
Figure 18: Map displaying the distribution of temperature observations, with a colour code that represents the BaSIC20 model vs. observation differences. The relation between differences and each colour coded range is displayed at the bottom of the figure.	29
Figure 19: Probability distribution of BaSIC20 model vs. observation differences in potential temperature (averages over top 100m). Values were aggregated in bins of 0.4K, and the amplitude is normalized by dividing the number of entries in each bin by the total no. of observations. The bias and standard deviation were +0.03K and 0.76K, respectively. Data from 12.558 profiles were included.	30
Figure 20: Scatter plot for averaged potential temperature from the upper 100m of the water column, for observations (horizontal axis) vs. BaSIC20 model results (vertical axis). The colour code corresponds to the corresponding salinity average in the observations. High salinity dots are plotted on top.	30
Figure 21: Same as Figure 18, but for salinity.	31
Figure 22: Same as Figure 19, but for salinity. Values were aggregated in bins of 0.06ppt. The bias and standard deviation were +0.051ppt and 0.631ppt, respectively.	31
Figure 23: Same as Figure 20, but for salinity. The colour code corresponds to observed temperature, with warm dots plotted on top.	32
Figure 24: Time series of sea ice area (integral of sea ice concentration) in the domain of the BaSIC20 model configuration. OSI SAF observations are displayed by the yellow line, while model results from BaSIC20 are shown by the blue line. Overall averages are (in Mkm <sup>2</sup> ) 8.40 (OSI SAF), and 8.60 (BaSIC20).	32
Figure 25: Same as Figure 24, but for time series of sea ice extent (area where the sea ice concentration exceeds 0.15). Overall averages are (in Mkm <sup>2</sup> ) 9.71 (OSI SAF), and 9.58 (BaSIC20).	33
Figure 26: Averaged surface currents over the simulation period 2000 – 2001.	34
Figure 27: Maximum current speed over the simulation period 2000 - 2001.	35
Figure 28: Maximum ice concentration for the model domain over the period 2000 - 2001. Note that this maximum concentration for each grid point, this did not necessarily happen at the same time	35
Figure 29: Same as for Figure 28, but minimum extent.	36
Figure 30: Position of stations for current measurements.	37
Figure 31: Frequency diagrams of current speed (in cm/s) over the years 2000 - 2001 in the Fugløya - Bjørnøya section at each station (CM1 - CM5). The left column shows results at 125m depth, and the right column shows results for the bottom depths. Red lines are observations and blue lines are the BaSIC4 model results.	38

Figure 32: Frequency diagrams of current direction over the years 2000 - 2001 in the Fugløya - Bjørnøya section at each station (CM1 - CM5). The left column shows results at 125m depth, and the right column shows results for the bottom depths. Red lines are observations and blue lines are the BaSIC4 model results. 39

Figure 33: Combined qq- and scatterplots for current speed (in cm/s) over the years 2000 - 2001 in the Fugløya - Bjørnøya section at each station (CM1 - CM5). Observations are along the horizontal axis and BaSIC4 model along the vertical axis. The left column shows results at 125m depth, and the right column shows results for the bottom depths. Green dots are the scatterplots, and blue "pluss-signs" indicate the qq-plots. 40

Figure 34: Maps displaying the distribution of temperature observations, with a colour code that represents the model vs. observation differences. The relation between differences and each colour coded range is displayed at the bottom of the figures. Results from BaSIC4 and SVIM4 are shown in the top and bottom panels, respectively. 41

Figure 35: Probability distributions of differences in potential temperature (averages over top 100m). Values were aggregated in bins of 0.4K, and the amplitude is normalized by dividing the number of entries in each bin by the total no. of observations. The bias and standard deviation in BaSIC4 (top panel) were -0.05K and 1.05K, respectively. The corresponding values in SVIM4 (bottom panel) were -0.61K and 1.27K. Data from 11.005 profiles were included. 42

Figure 36: Scatter plots for averaged potential temperature from the upper 100m of the water column, for observations (horizontal axis) vs. model results (vertical axis). The colour code corresponds to the corresponding salinity average in the observations. High salinity dots are plotted on top. Results from BaSIC4 and SVIM4 are shown in the top and bottom panels, respectively. 43

Figure 37: Same as Figure 34, but for salinity offset. BaSIC4 in top panel and SVIM4 in bottom panel. 44

Figure 38: Same as Figure 35, but for salinity. Values were aggregated in bins of 0.06ppt. The bias and standard deviation in BaSIC4 were +0.339ppt and 1.202ppt, respectively. The corresponding values in SVIM4 were +0.114ppt and 1.018ppt. 45

Figure 39: Same as Figure 36, but for salinity. The colour code corresponds to observed temperature, with warm dots plotted on top. 46

Figure 40: Time series of sea ice area (integral of sea ice concentration) in the domain of the BaSIC4 and SVIM4 model configurations. OSI SAF observations are displayed by the yellow line, while model results from BaSIC4 and SVIM4 are shown by the blue and black lines, respectively. Overall averages are (in  $\text{Mkm}^2$ ) 2.21 (OSI SAF), 2.11 (BaSIC4), and 2.32 (SVIM4). 47

Figure 41: Same as Figure 40, but for time series of sea ice extent (area where the sea ice concentration exceeds 0.15). Overall averages are (in  $\text{Mkm}^2$ ) 2.68 (OSI SAF), 2.63 (BaSIC4), and 2.75 (SVIM4). 47

Figure 42: Comparison of current speed from BaSIC20 and BaSIC2 models. For detailed explanations, see page 48. 49

Figure 43: Comparison of current speed form BaSIC20 and BaSIC4 models. For detailed explanaitons, see page 48. 50

Figure 44: Comparison of current speed form BaSIC4 and BaSIC2 models. For detailed explanaitons, see page 48. 51

## List of tables

Table 1: Available measurements for each site between Fugløya and Bjørnøya for the year 2000 - 2011 at 50m and the bottom depth. 21

Table 2: Fluxes through the different sections. The first column is the mean BaSIC20 flux in the main flow direction, pluss/minus one standard deviation. The second column is the net flux with standard deviation. The third column is net SVIM flux values. The last column shows observation based values from the literature. The SVIM4 and literature values are from the SVIM validation report (Lien et al., in press). The BaSIC20 run underestimates the Atlantic flow into the Nordic Seas, but does a better job for the East Greenland Current.27

Table 3: Available measurements for each site between Fugløya and Bjørnøya for the year 2000 - 2001 at 125m and the bottom depth. 37



# 1 Introduction

This is an addendum to MET report no. 12/2013. Presented and explained are the new model grid configuration and results emanating from a final trial hindcast.

The decision to perform a final trial hindcast was made since we were not satisfied with the results derived earlier and reported in MET report no 12/2013. In particular we were unhappy with the results for ocean currents. As a consequence the new and final hindcast utilizes a new grid configuration and another vertical mixing scheme. The new grid configuration consists of the BaSIC20 grid (20 km mesh size) and the BaSIC4 (4 km mesh size) as displayed in Figure 1.

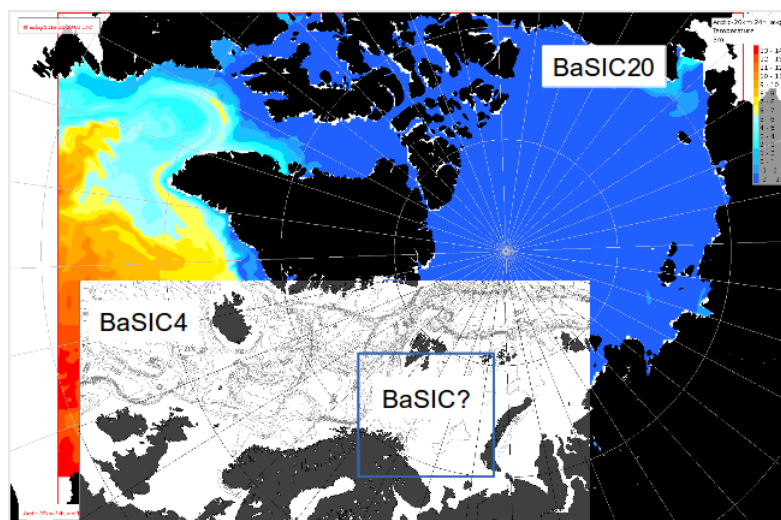


Figure 1: The new grid configuration used in the final trial hindcast

BaSIC4 is one-way nested into BaSIC20 so that it makes use of the BaSIC20 results on its open boundaries. At the open boundaries of the BaSIC20 grid we use results from the global UK Met Office model FOAM. FOAM provides reanalysed data from 1993 and onwards. Note that BaSIC20 extends into the Bering Sea, so that FOAM results are used at the open boundary

in the Bering Sea as well as along the North Atlantic open boundary. The BaSIC4 grid conforms to the earlier SVIM4 grid, and hence BaSIC4 results may be compared to the SVIM4 results.

In the work following MET report no. 12/2013, modifications of the experiment design were tested. Results obtained by replacing the use of SVIM results at the open boundary with a dedicated 20km model configuration were encouraging, although the new configuration was not fully consistent with the original. Furthermore, initial test with an alternative mixing scheme (the K-Profile Parameterization; KPP) revealed little change when compared to a parallel experiment with the original scheme (Generic Length Scale; GLS). However, other tests carried out at MET Norway indicate that GLS has too much mixing near steep topography. We also discovered that our initial implementation of KPP in BaSIC suffered from an incomplete implementation. Results which are reported here, with a more complete implementation of KPP strongly suggest that changing from GLS to KPP has a positive impact on the model results for velocity.

The BaSIC20 grid was utilized to provide an 18 year hindcast starting January 1, 1993 and ending December 31, 2010. Atmospheric input was provided by the ERA40 reanalysis extended with the ERA interim data. Furthermore we utilized the BaSIC4 grid to provide a three year hindcast starting January 1, 1999 and ending December 31, 2001, in which we used results from the BaSIC20 hindcast at the open boundaries. As atmospheric input we switched to the NORA10 data.

Regarding validation, the observations we have used is hydrography (temperature, salinity), sea-ice and currents from 2000 and 2001. The hydrography data are taken from the World Ocean Database (Boyer et al., 2009). Validation is performed for quantities that have been averaged over the upper 100m of the water column (or top to bottom in regions where the depth is smaller than 100m). Statistics have been produced for differences between observations and corresponding model results, and positive numbers correspond to larger values in model results than in observations. Observations of sea-ice (concentration) were derived from satellite imagery through the Ocean and Sea Ice Satellite Application Facility (OSI SAF) High Latitude Processing Center (Andersen et al., 2012; Eastwood et al., 2011). Sea ice concentrations have been interpolated/extrapolated onto regions where observations were originally discarded due to cloud contamination. Ocean current observations for the five current meters at the Barents Sea opening were provided by IMR and are the same as those used in MET report 12/2013.

The report is organized as follows. In Section 2 we first briefly present some model results from the BaSIC20 grid hindcast (Section 2.1), which is followed by a validation (Section 2.2) in terms of currents, temperature, salinity and sea ice. In Section 3 we focus on results from the BaSIC4 grid and first present the model results (Section 3.1) followed by the validation results (Section 3.2). Note that the validation of currents also includes qq-plots and scatter plots regarding currents in the Barents Sea opening (Figure 8). Section 4 presents the current speeds from model grids of different resolution or mesh size as qq-plots against current speed observations in the Barents Sea opening. These results are added to indicate what is gained in terms of current speed when progressing towards higher resolution (smaller mesh size). We end the report with some final remarks, conclusions and recommendations (Section 4).

## 2 BaSIC20 model

### 2.1 Model results

#### 2.1.1 Currents

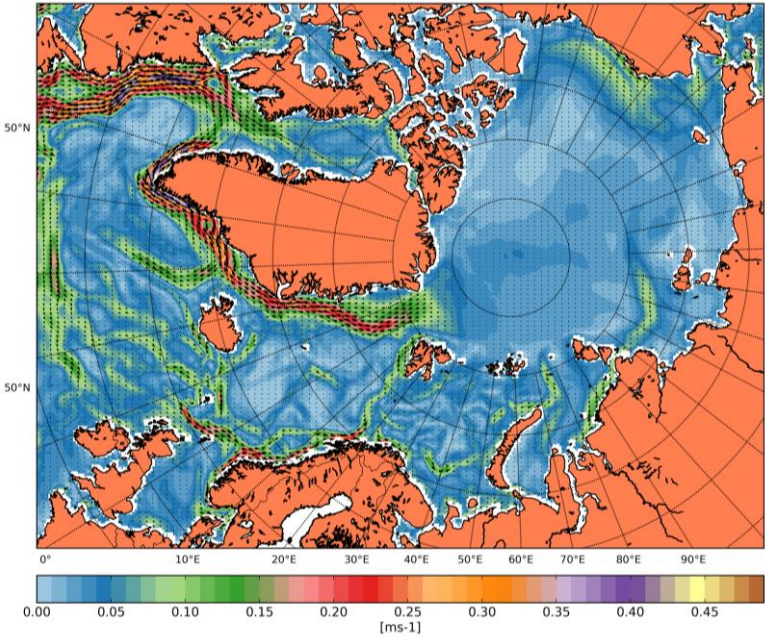


Figure 2: Averaged surface currents over the simulation period 1993 - 2010.

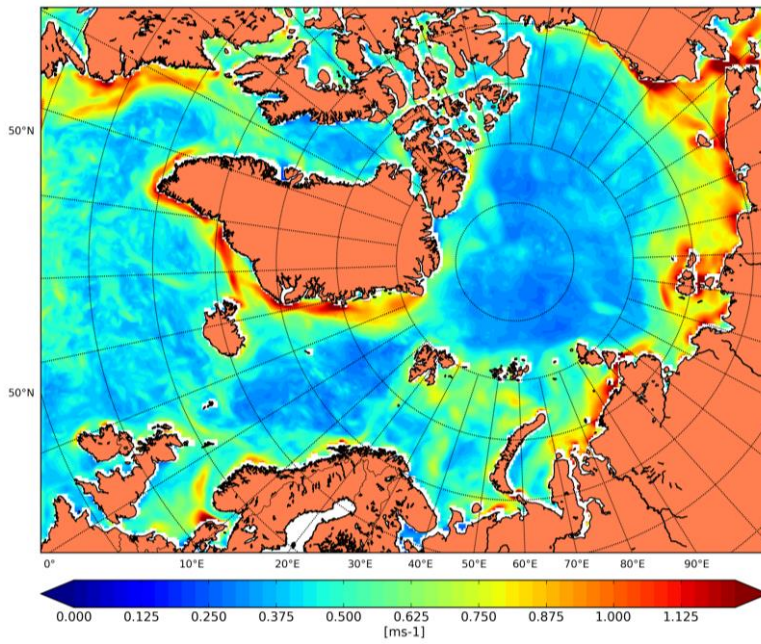


Figure 3: Maximum current speed over the simulation period 1993 - 2010.

## 2.1.2 Sea ice

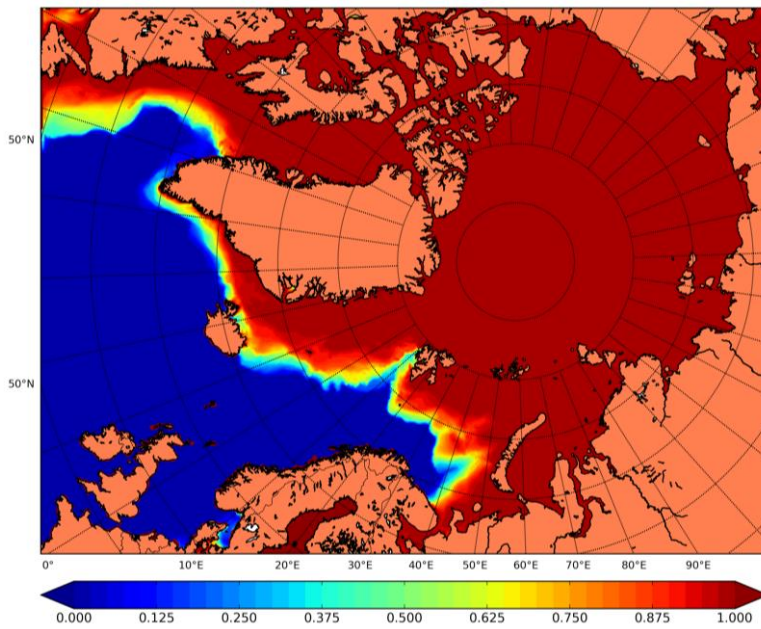


Figure 4: Maximum ice concentration for the model domain over the period 1995 - 2010. Note that this maximum concentration for each grid point, this did not necessarily happen at the same time.

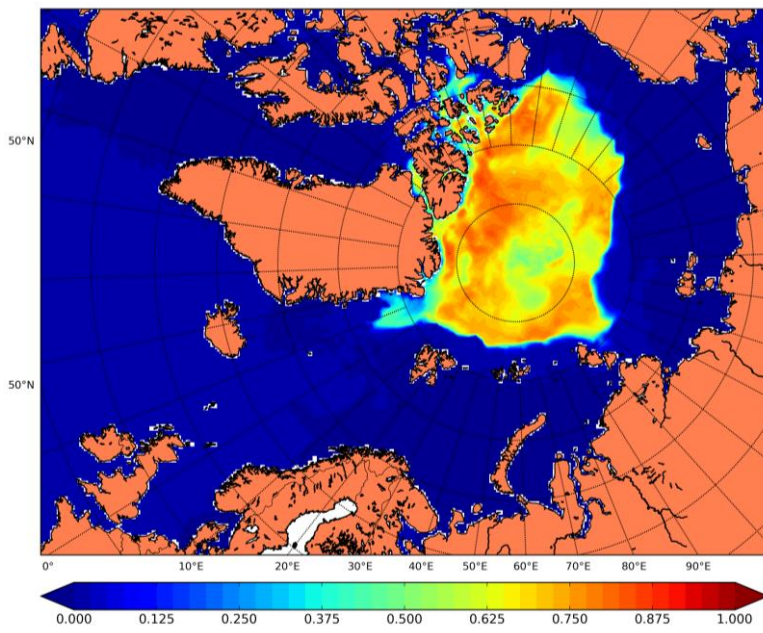


Figure 5: Same as Figure 4, but minimum extent.

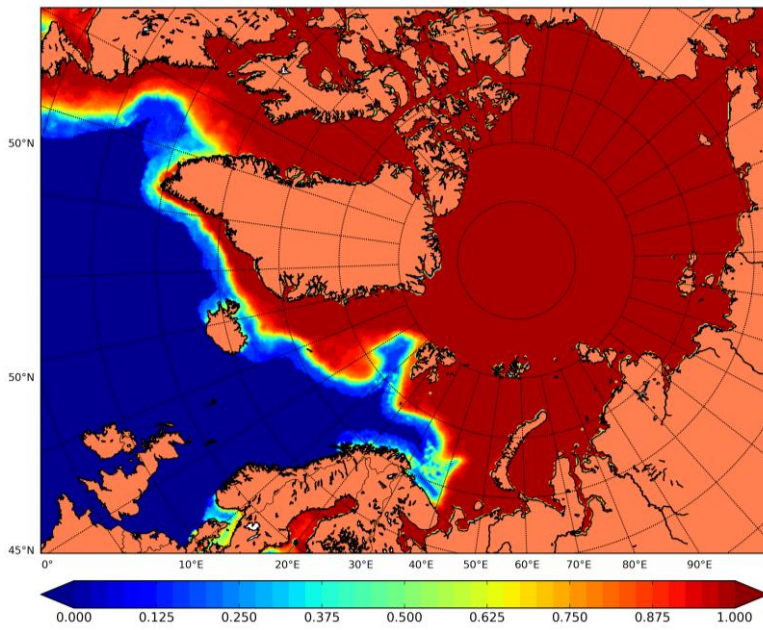


Figure 6: Same as Figure 4, but based on OSISAF satellite observations.

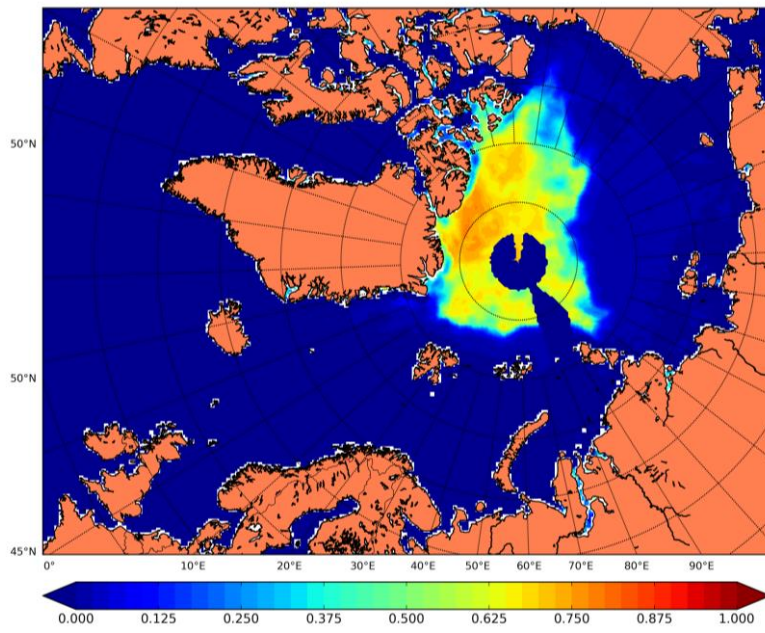


Figure 7: Same as Figure 6, but for minimum extent.

## 2.2 Validation

### 2.2.1 Currents

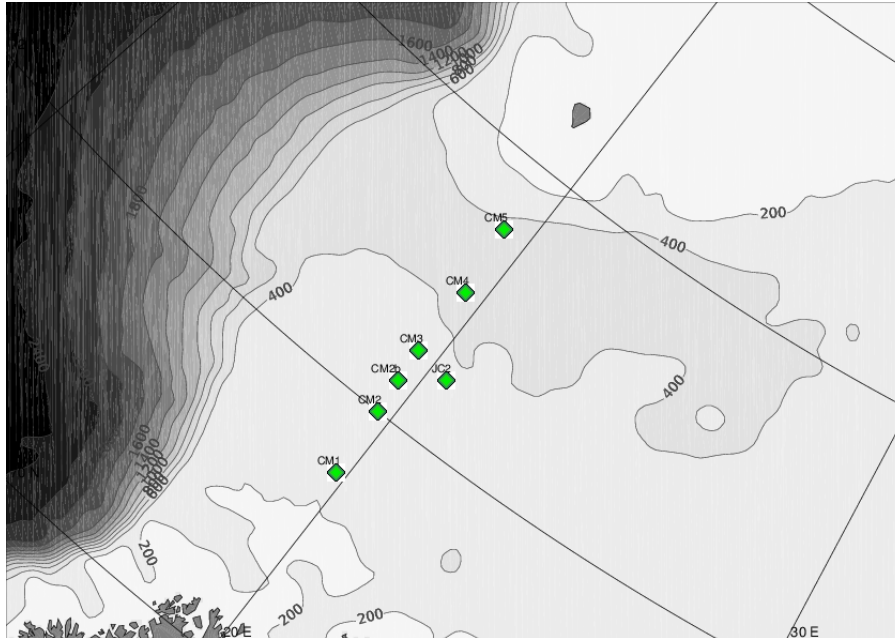


Figure 8: Position of stations for current measurements.

2000 - 2011				
Name	N		Bottom depth	
	50m	Bottom	Observation	Model (Real depth)
<b>CM1</b>	1802	2370	212m	212m (263m)
<b>CM2</b>	3257	4179	294m	294m (315m)
<b>CM3</b>	3228	3976	373m	360m (-)
<b>CM4</b>	2617	3754	401m	401m (-)
<b>CM5</b>	2541	2886	464m	370m (-)

Table 1: Available measurements for each site between Fugløya and Bjørnøya for the year 2000 - 2011 at 50m and the bottom depth.

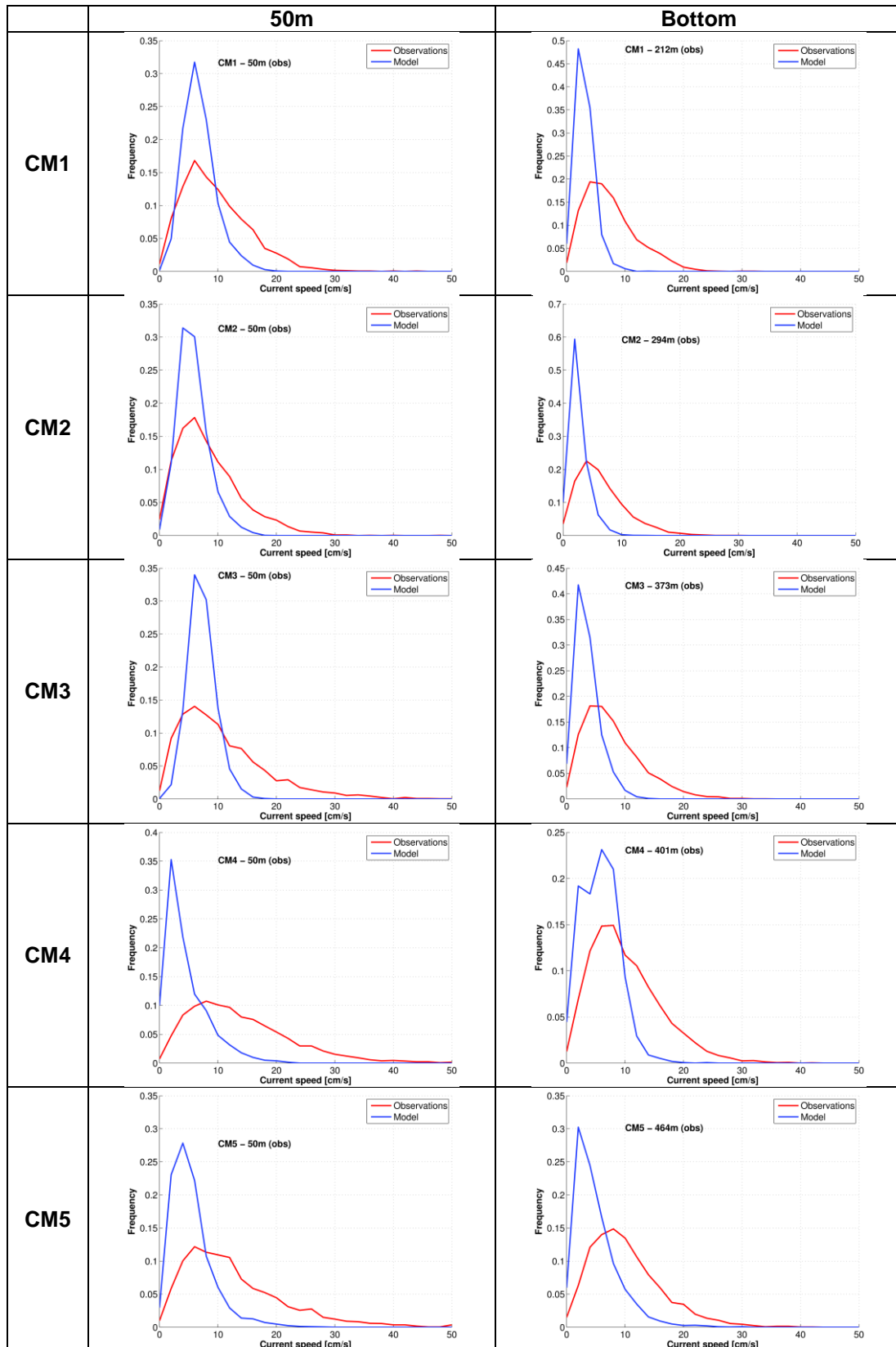


Figure 9: Frequency diagrams of current speed (in cm/s) over the years 2000 - 2011 in the Fugløya - Bjørnøya section at each station (CM1 - CM5). The left column shows results at 50m depth, and the right column shows results for the bottom depths. Red lines are observations and blue lines are the BaSIC20 model results.

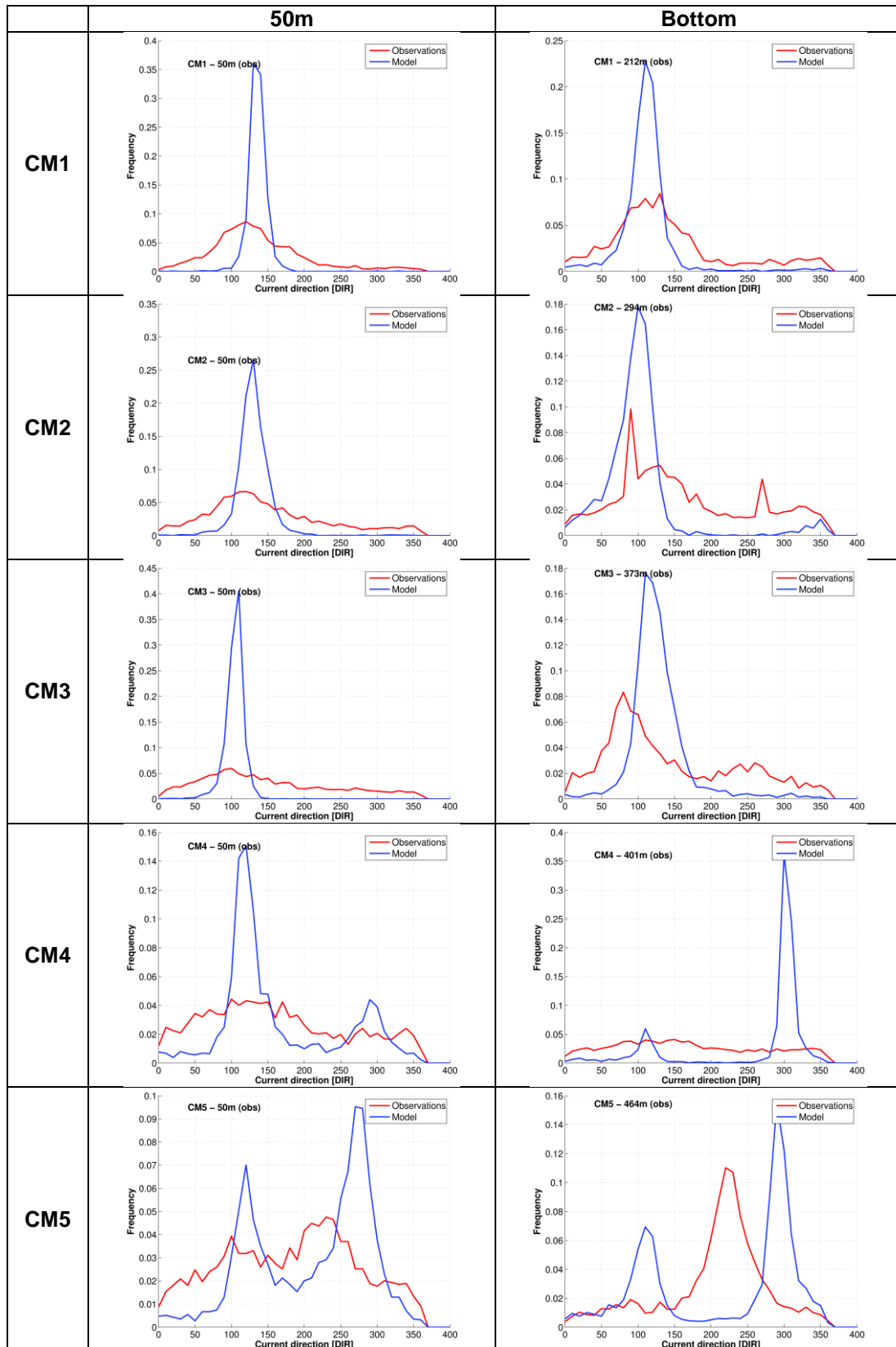


Figure 10: Frequency diagrams of current direction over the years 2000 - 2011 in the Fugløya - Bjørnøya section at each station (CM1 - CM5). The left column shows results at 50m depth, and the right column shows results for the bottom depths. Red lines are observations and blue lines are the BaSIC20 model results.

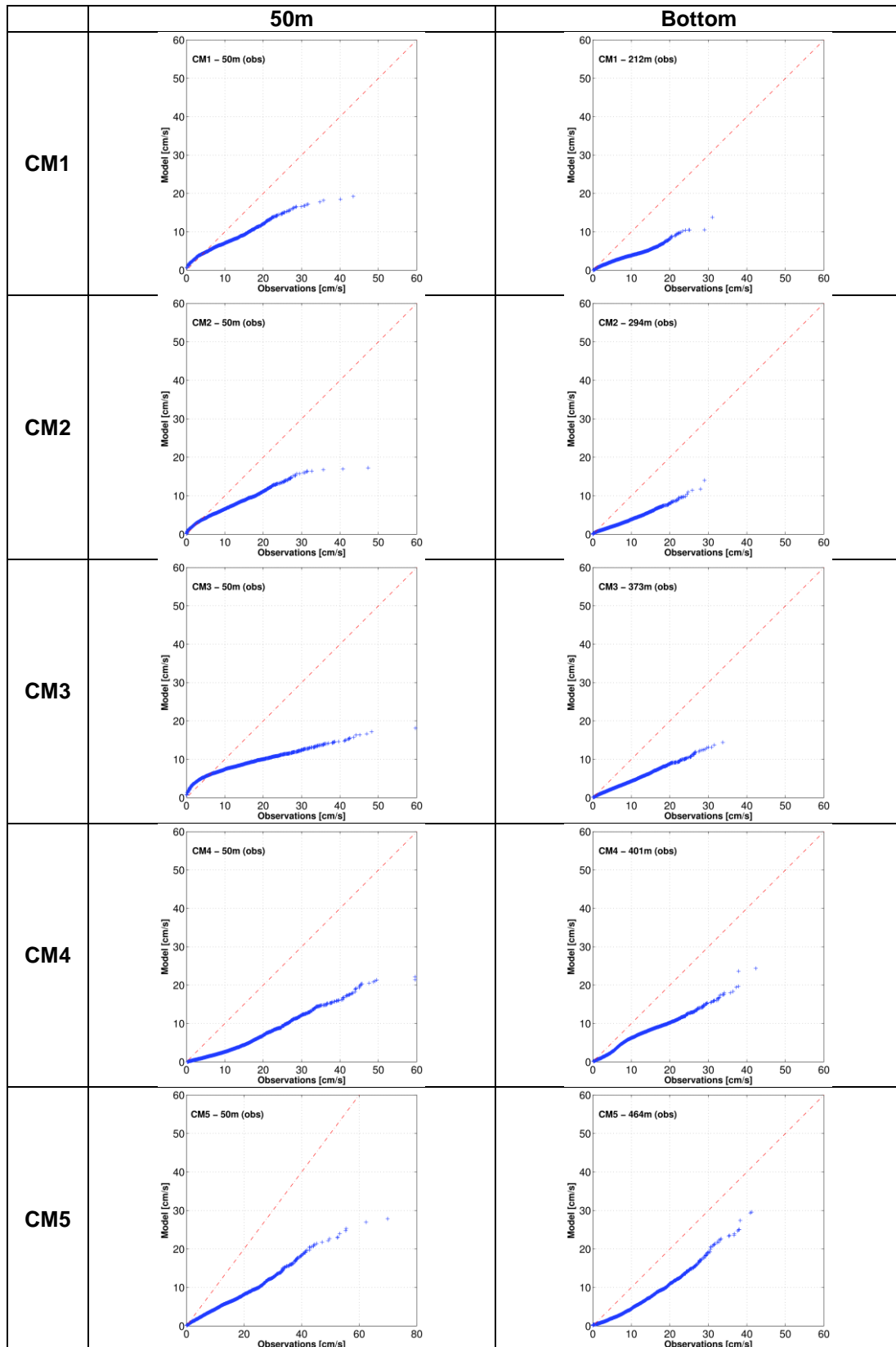


Figure 11: Frequency diagrams of current direction over the years 2000 - 2011 in the Fugløya - Bjørnøya section at each station (CM1 - CM5). The left column shows results at 50m depth, and the right column shows results for the bottom depths. Red lines are observations and blue lines are the BaSIC20 model results.

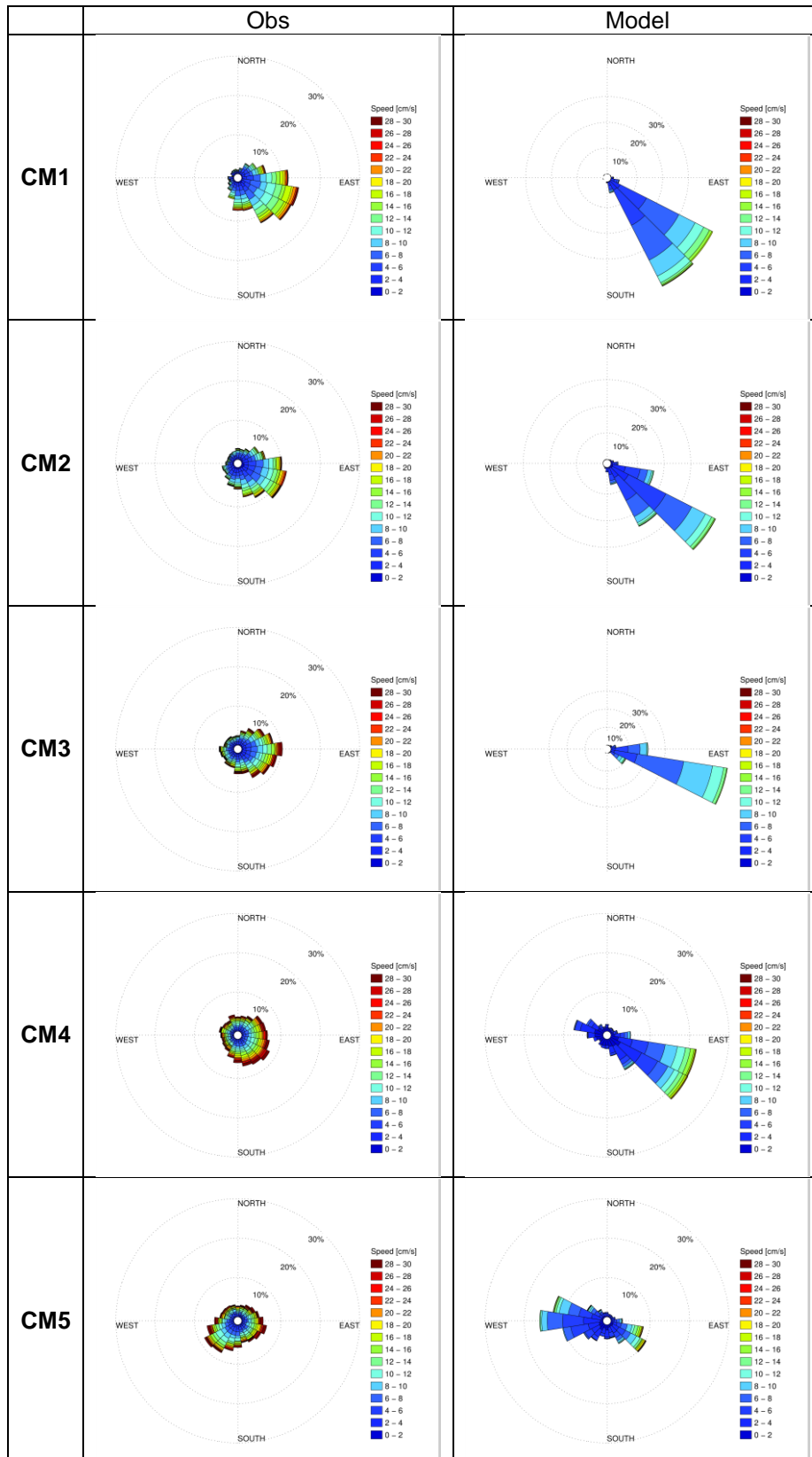


Figure 12: Distribution of current direction together with current speed for the year 2000 -2011 in the Fugløya-Bjørnøya section at 50m depth at station CM1 through CM5. The first column show results for the current meter data and the second column the BaSIC20 model currents.

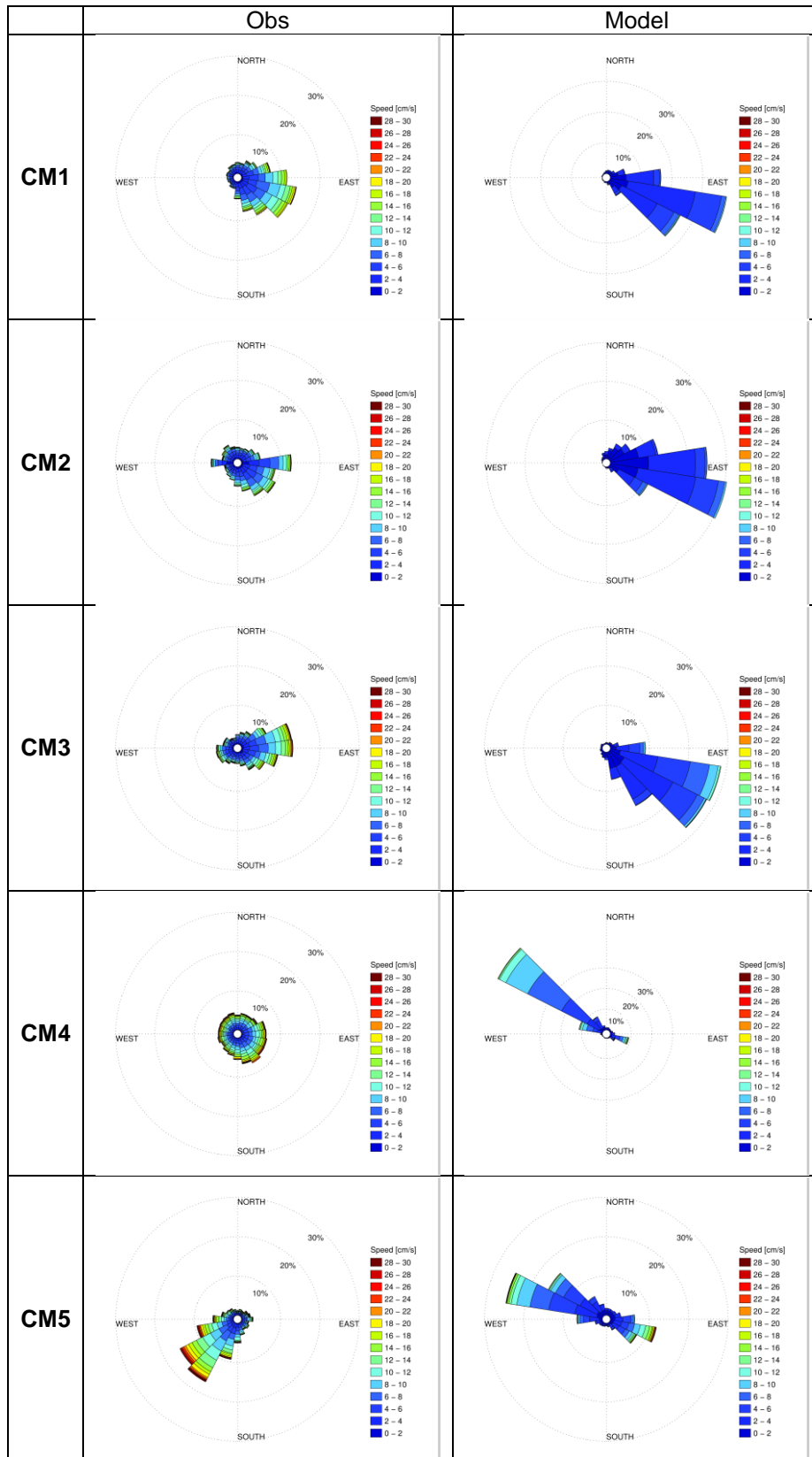


Figure 13: Same as Figure 12, but for the bottom.

## 2.2.2 Volume fluxes

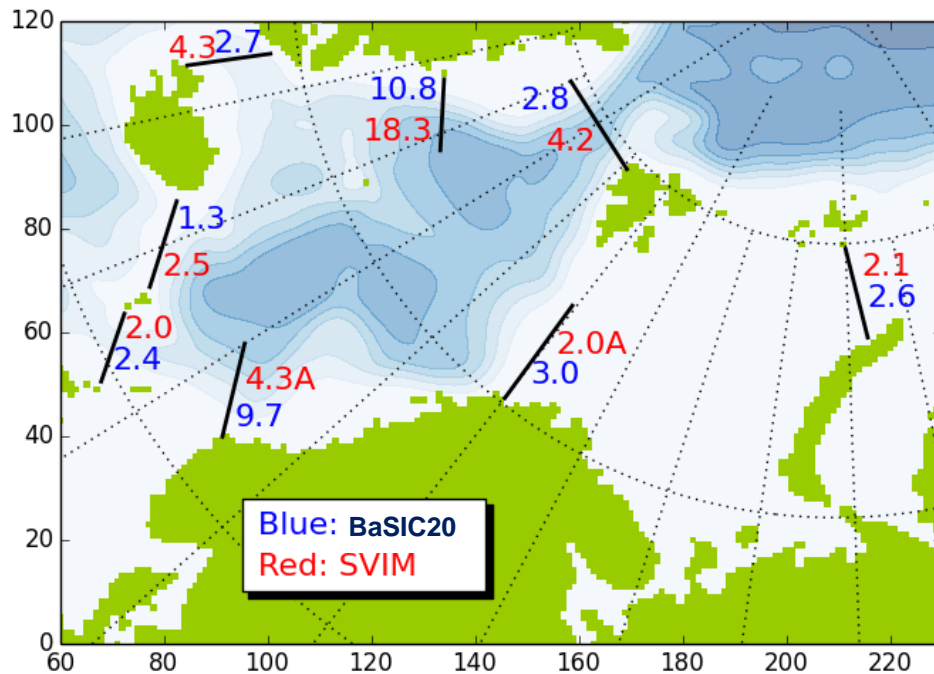


Figure 14: Overview of the mean volume fluxes in Sverdrup trough different sections. Values in blue are from the BaSIC20 simulation and the red values from the SVIM4 simulation. Red values with an "A" represents Atlantic Water only.

Section	BaSIC20 main direction	BaSIC20 net	SVIM4 net	Observations literature
Icel. – Faeros	3.0 ± 0.9	1.3 ± 0.7	2.5	3.5 – 4.6
F-Sh. Channel	5.5 ± 1.2	2.4 ± 1.8	2.4	2.7 – 4.1
Svinøy-NW	11.2 ± 3.6	9.7 ± 4.5	4.3 A	2.7 – 5.7 A
Bar. Sea. Op.	3.6 ± 1.2	3.0 ± 1.3	2.0 A	1.5 – 2.0 A
Nov.Z – Fr.Jo.	3.1 ± 0.8	2.6 ± 1.1	2.1	1.1 – 2.1
Fram Strait	11.2 ± 2.6	2.8 ± 1.3	4.2	-0.7 – 4.2
East Gr. Current	12.9 ± 4.2	10.8 ± 5.0	18.3	21 – 29
Denmark Str.	4.8 ± 1.1	2.7 ± 1.4	4.3	2.7

Table 2: Fluxes through the different sections. The first column is the mean BaSIC20 flux in the main flow direction, plus/minus one standard deviation. The second column is the net flux with standard deviation. The third column is net SVIM4 flux values. The last column shows observation based values from the literature. The SVIM4 and literature values are from the SVIM validation report (Lien et al., in press). The BaSIC20 run underestimates the Atlantic flow into the Nordic Seas, but does a better job for the East Greenland Current.

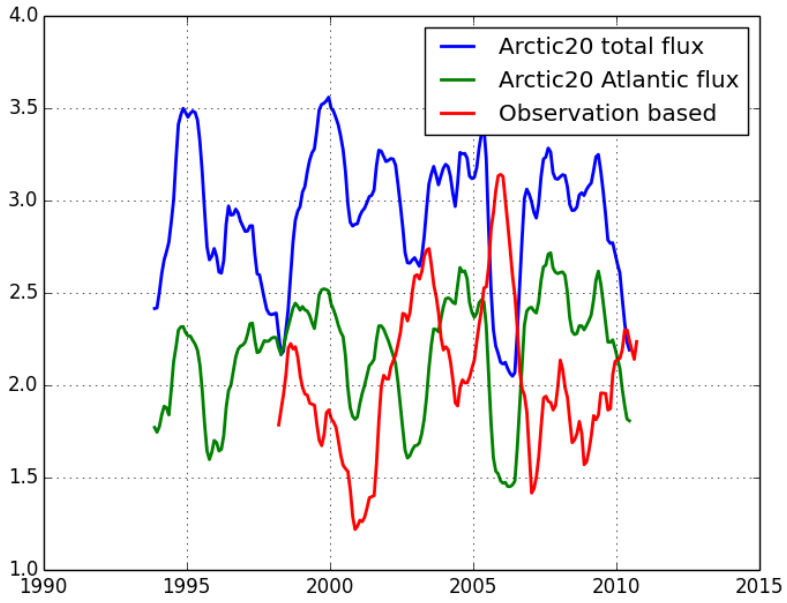


Figure 15: Barents Sea Opening (BSO) volume flux, one year moving average.

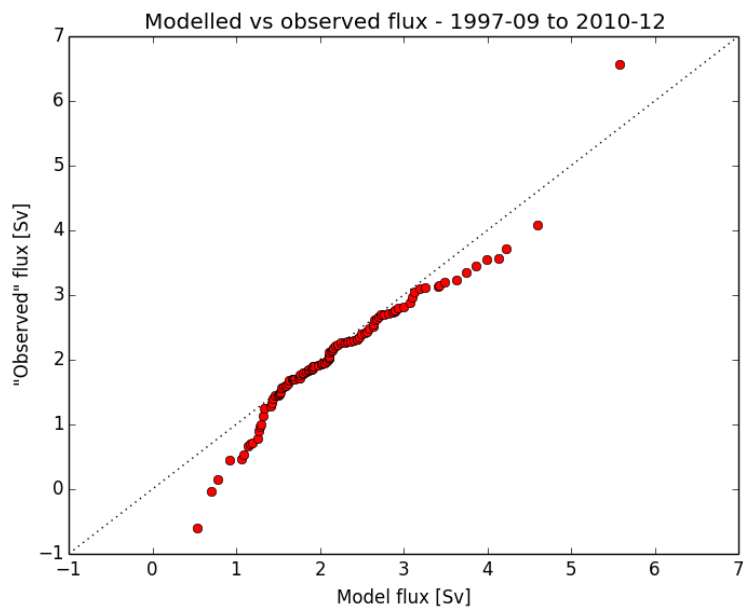


Figure 16: Qq-plot of Atlantic volume flux in BSO as monthly values.

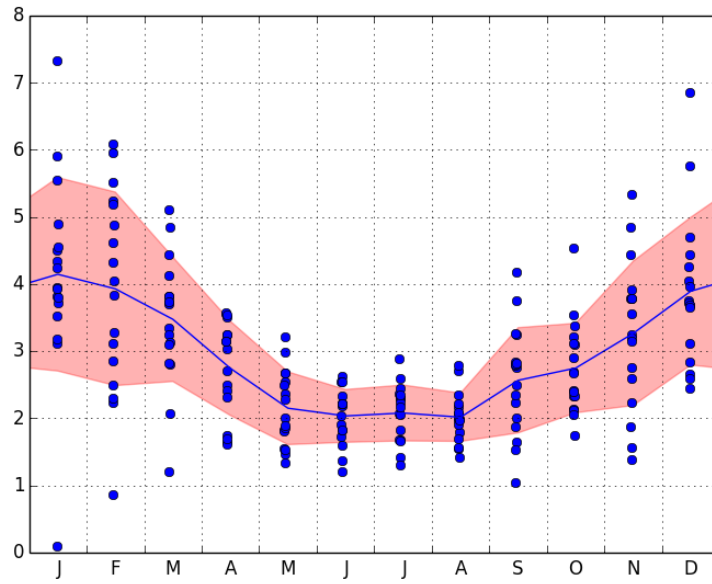


Figure 17: Seasonal variability of BSO volume flux.

### 2.2.3 Temperature and salinity

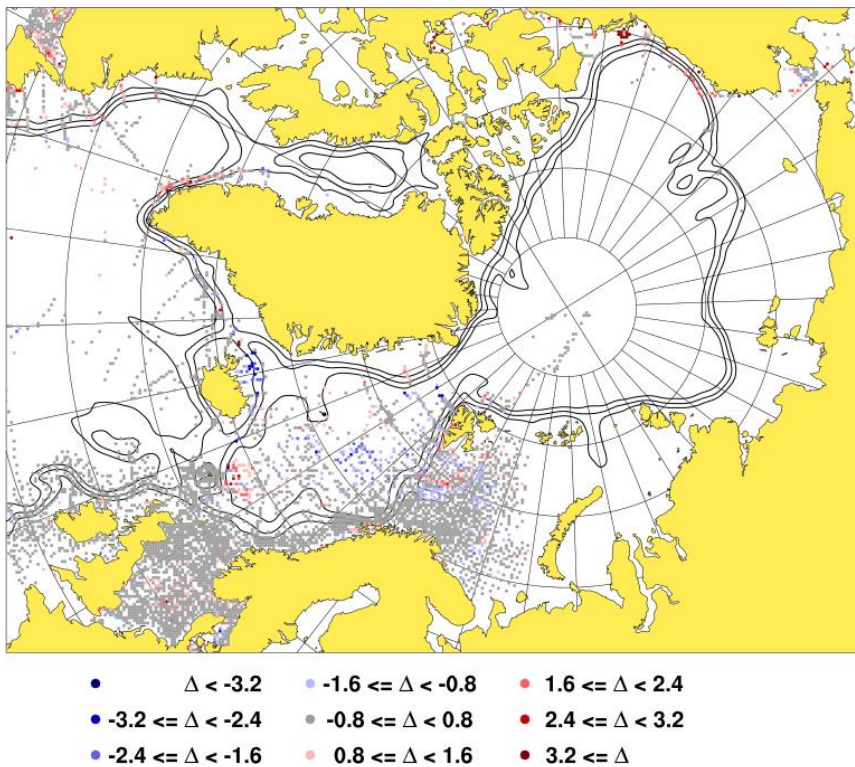


Figure 18: Map displaying the distribution of temperature observations, with a colour code that represents the BaSIC20 model vs. observation differences. The relation between differences and each colour coded range is displayed at the bottom of the figure.

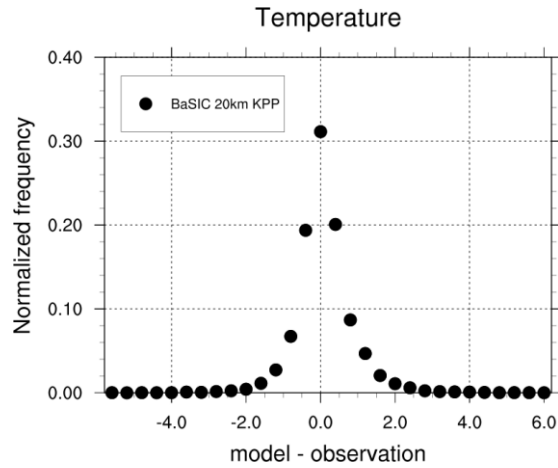


Figure 19: Probability distribution of BaSIC20 model vs. observation differences in potential temperature (averages over top 100m). Values were aggregated in bins of 0.4K, and the amplitude is normalized by dividing the number of entries in each bin by the total no. of observations. The bias and standard deviation were +0.03K and 0.76K, respectively. Data from 12.558 profiles were included.

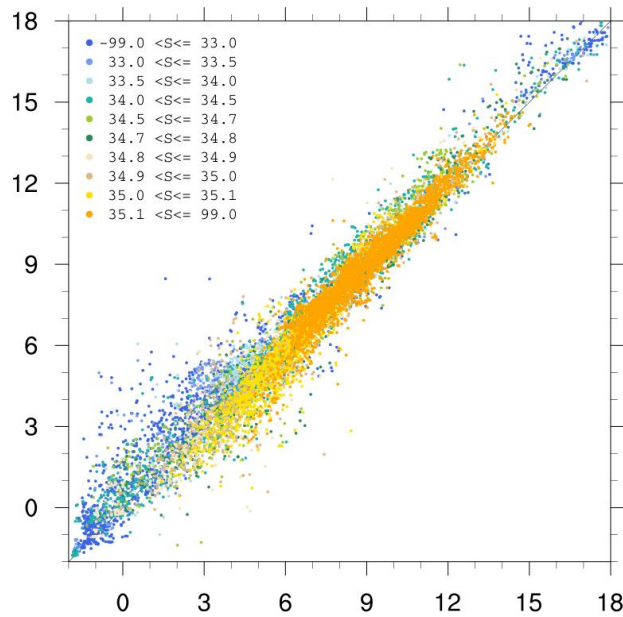


Figure 20: Scatter plot for averaged potential temperature from the upper 100m of the water column, for observations (horizontal axis) vs. BaSIC20 model results (vertical axis). The colour code corresponds to the corresponding salinity average in the observations. High salinity dots are plotted on top.

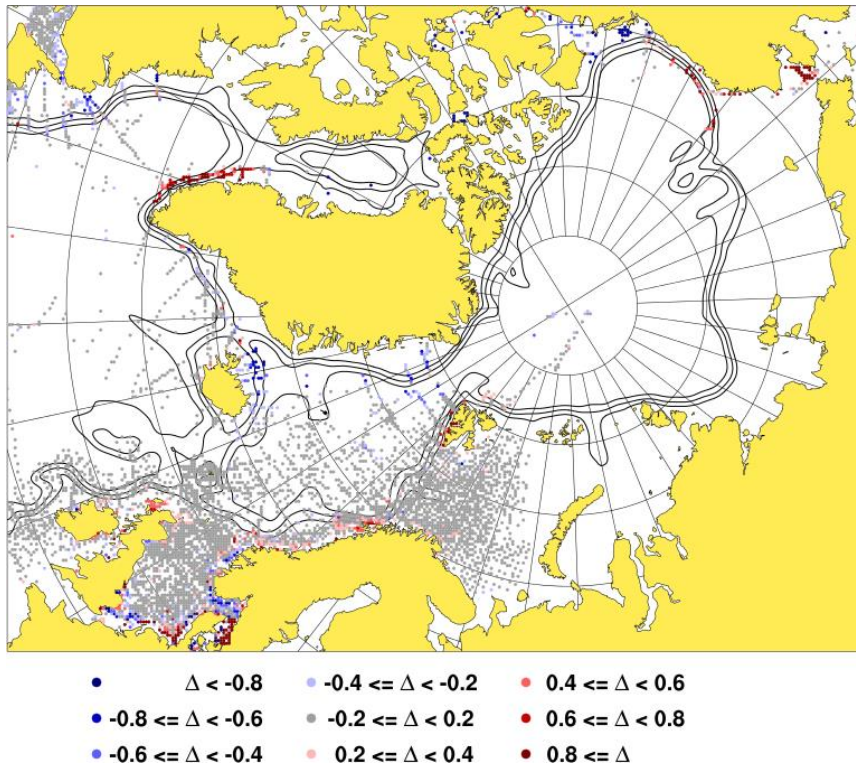


Figure 21: Same as Figure 18, but for salinity.

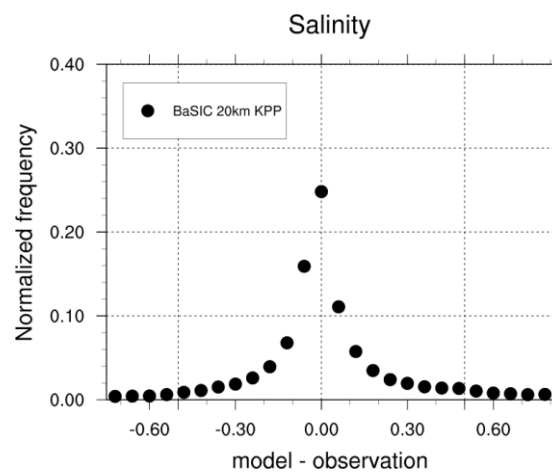


Figure 22: Same as Figure 19, but for salinity. Values were aggregated in bins of 0.06ppt. The bias and standard deviation were +0.051ppt and 0.631ppt, respectively.

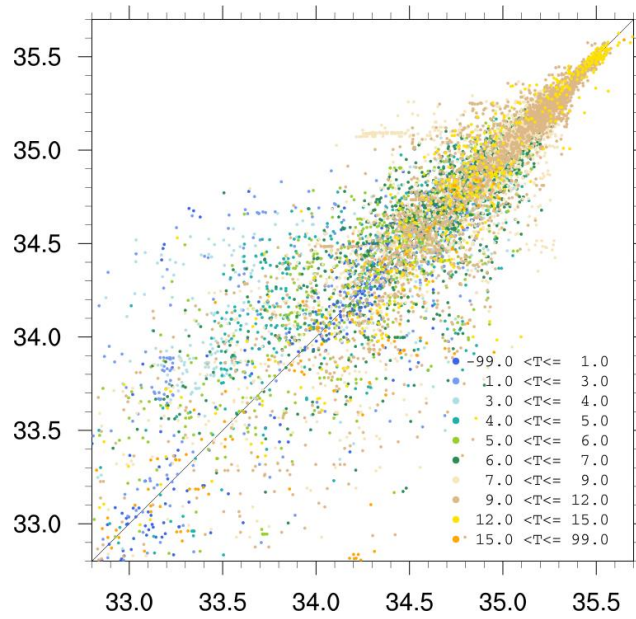


Figure 23: Same as Figure 20, but for salinity. The colour code corresponds to observed temperature, with warm dots plotted on top.

## 2.2.4 Sea ice

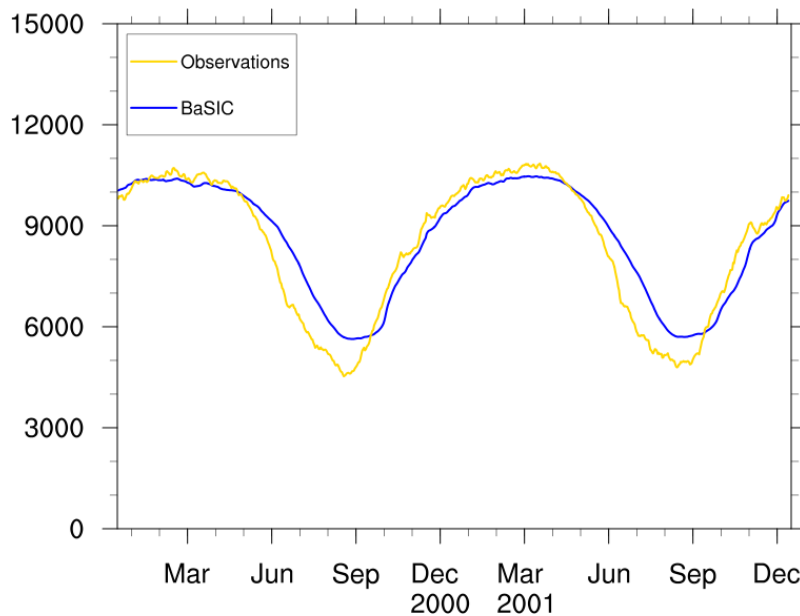


Figure 24: Time series of sea ice area (integral of sea ice concentration) in the domain of the BaSIC20 model configuration. OSI SAF observations are displayed by the yellow line, while model results from BaSIC20 are shown by the blue line. Overall averages are (in  $Mkm^2$ ) 8.40 (OSI SAF), and 8.60 (BaSIC20).

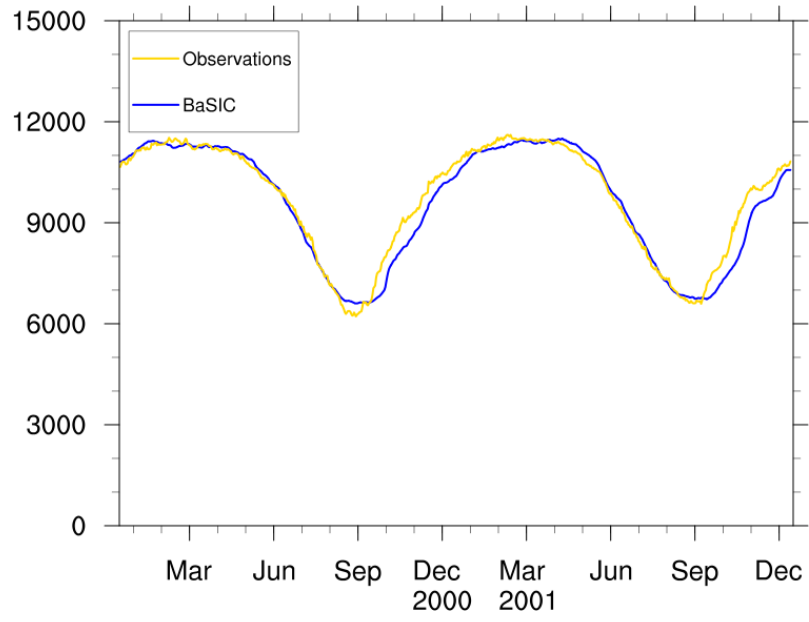


Figure 25: Same as Figure 24, but for time series of sea ice extent (area where the sea ice concentration exceeds 0.15). Overall averages are (in Mkm<sup>2</sup>) 9.71 (OSI SAF), and 9.58 (BaSIC20).

### 3 BaSIC4 model

#### 3.1 Model results

##### 3.1.1 Currents

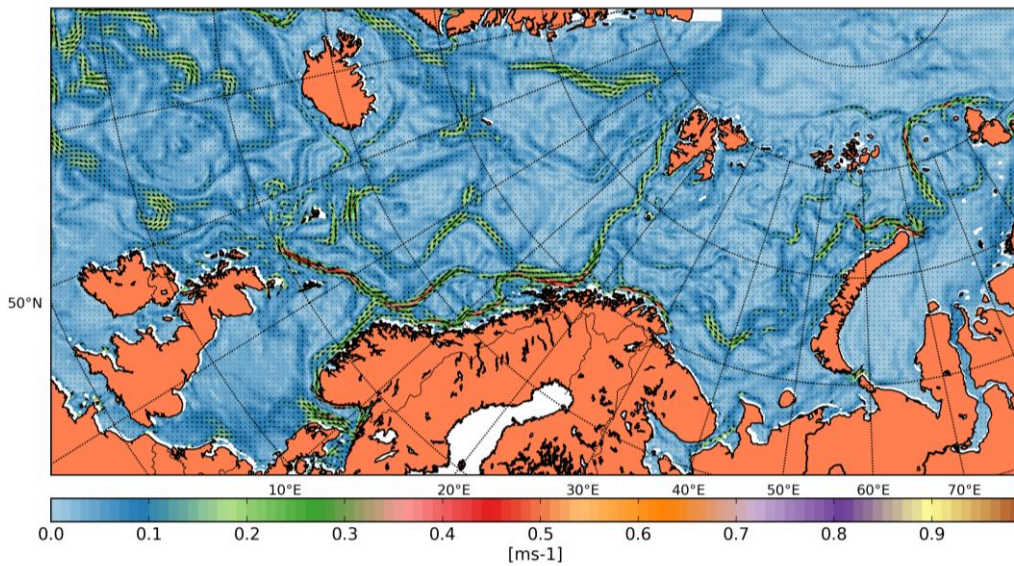


Figure 26: Averaged surface currents over the simulation period 2000 – 2001.

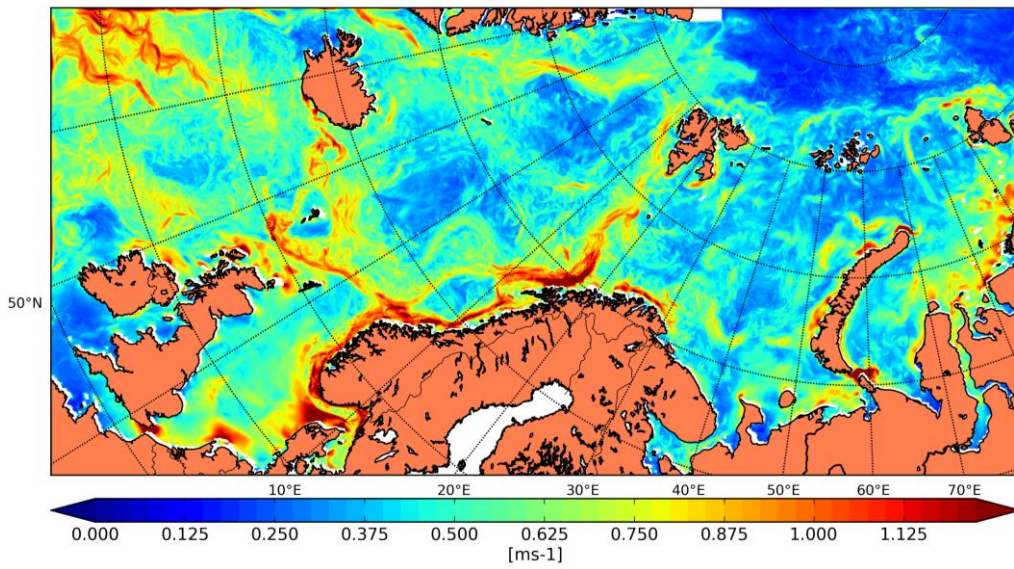


Figure 27: Maximum current speed over the simulation period 2000 - 2001.

### 3.1.2 Sea ice

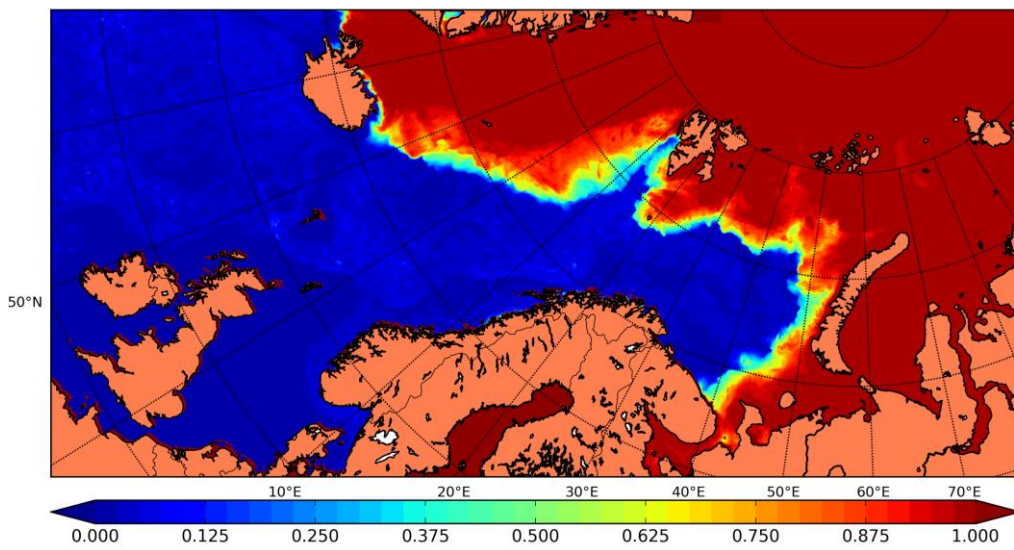


Figure 28: Maximum ice concentration for the model domain over the period 2000 - 2001. Note that this maximum concentration for each grid point, this did not necessarily happen at the same time

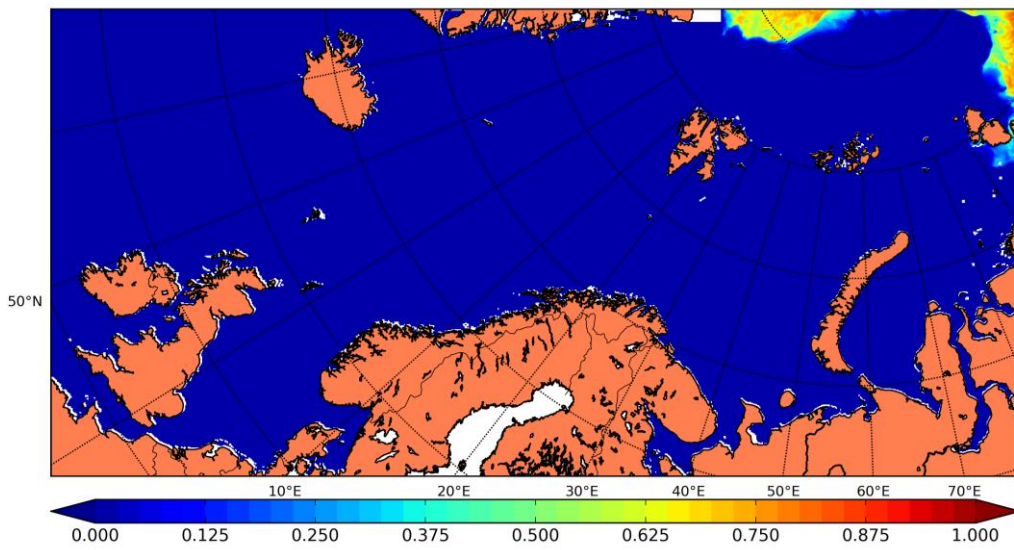


Figure 29: Same as for Figure 28, but minimum extent.

## 3.2 Validation

### 3.2.1 Currents

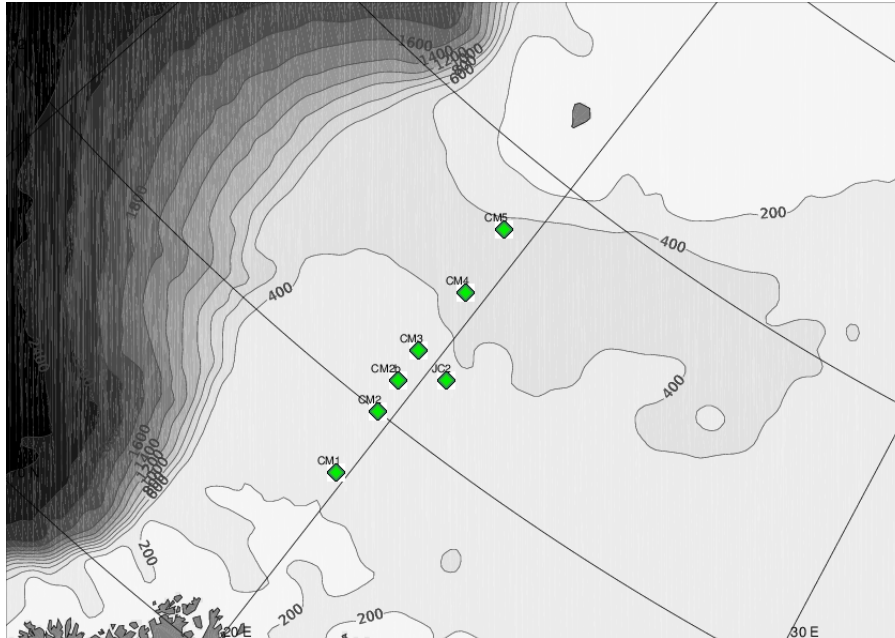


Figure 30: Position of stations for current measurements.

2000 - 2001				
Name	N		Bottom depth	
	125m	Bottom	Observation	Model (Real depth)
<b>CM1</b>			212m	m (263m)
<b>CM2</b>			294m	m (315m)
<b>CM3</b>			373m	m (-)
<b>CM4</b>			401m	m (-)
<b>CM5</b>			464m	m (-)

Table 3: Available measurements for each site between Fugløya and Bjørnøya for the year 2000 - 2001 at 125m and the bottom depth.

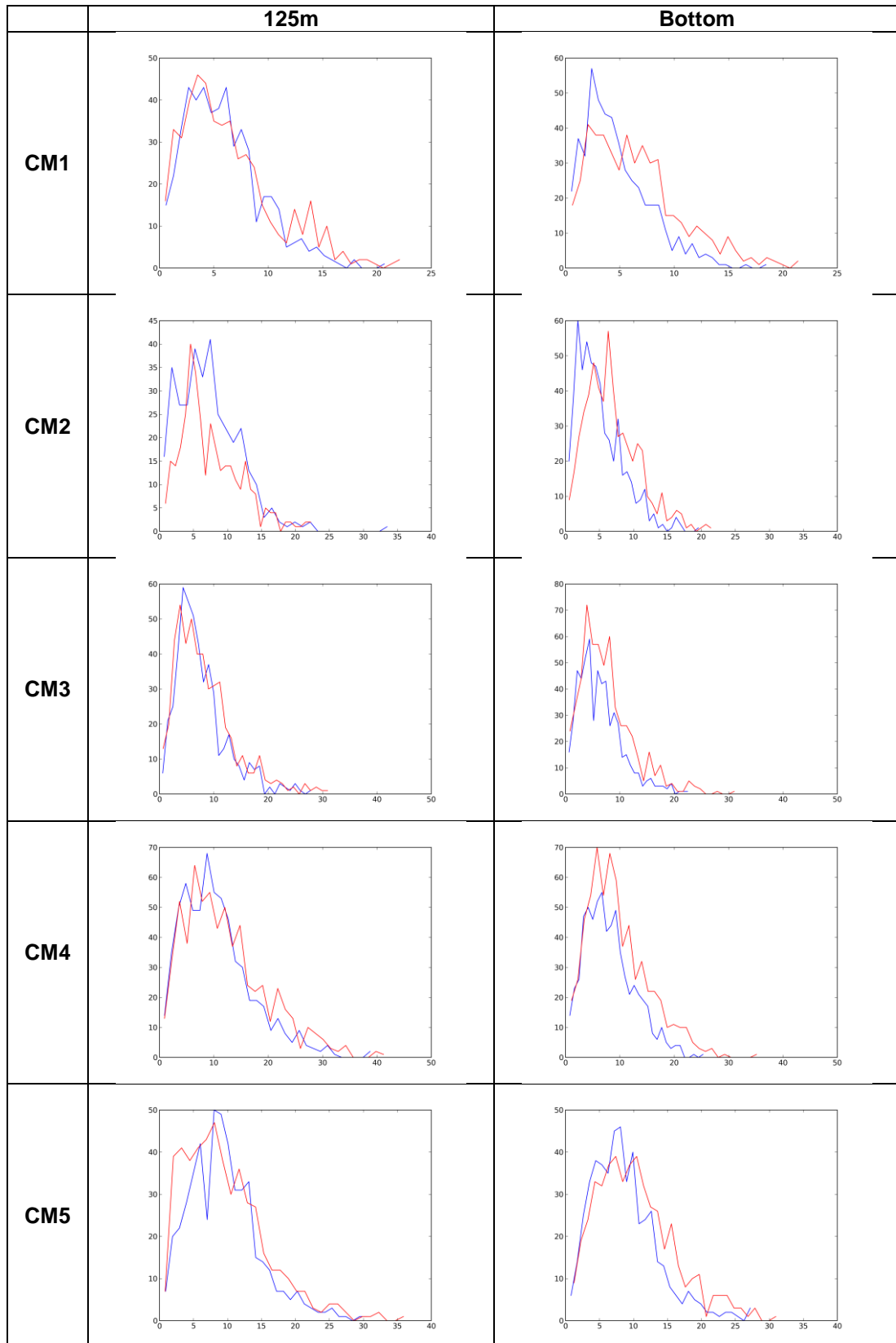


Figure 31: Frequency diagrams of current speed (in cm/s) over the years 2000 - 2001 in the Fugløya - Bjørnøya section at each station (CM1 - CM5). The left column shows results at 125m depth, and the right column shows results for the bottom depths. Red lines are observations and blue lines are the BaSIC4 model results.

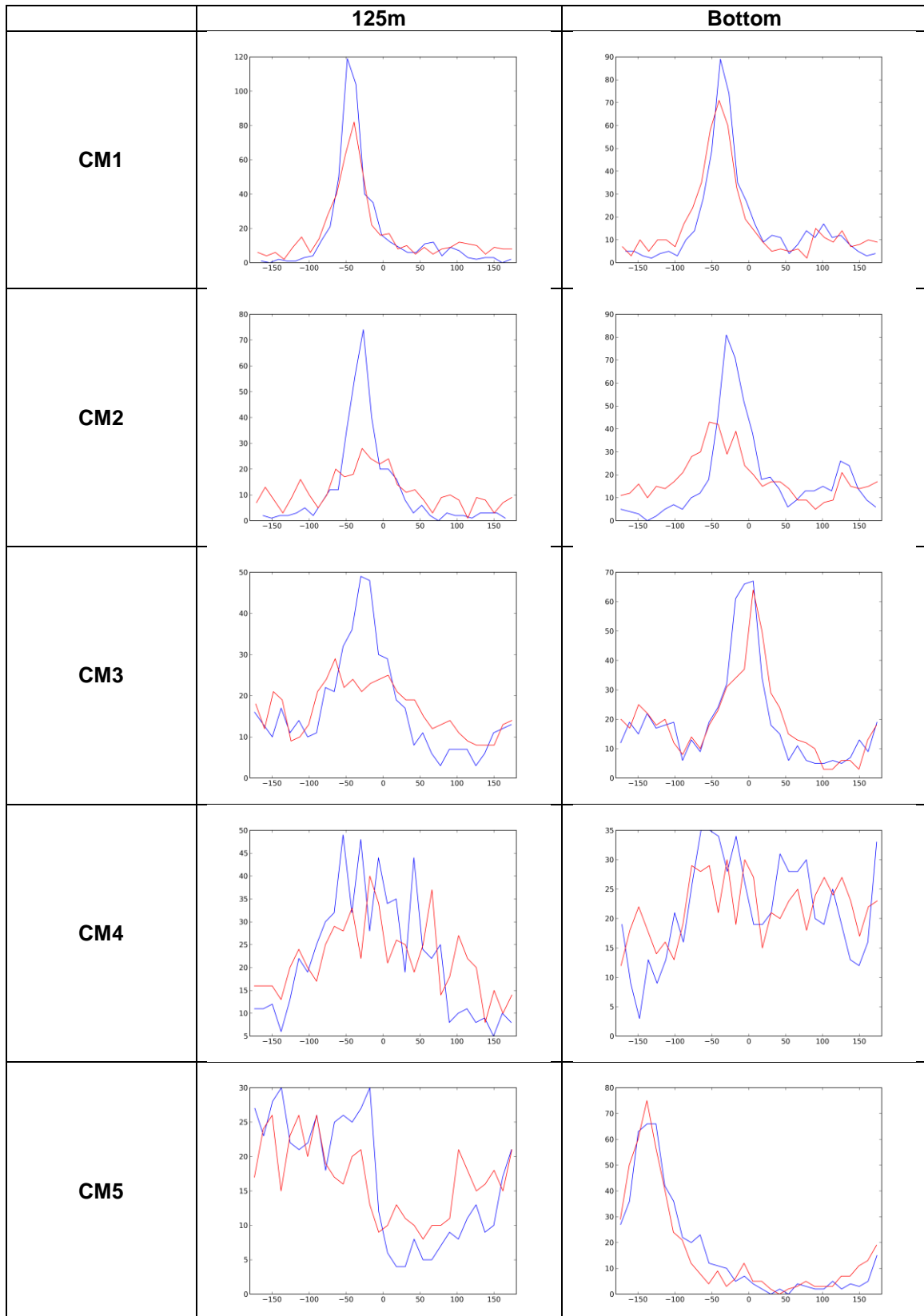


Figure 32: Frequency diagrams of current direction over the years 2000 - 2001 in the Fugløya - Bjørnøya section at each station (CM1 - CM5). The left column shows results at 125m depth, and the right column shows results for the bottom depths. Red lines are observations and blue lines are the BaSIC4 model results.

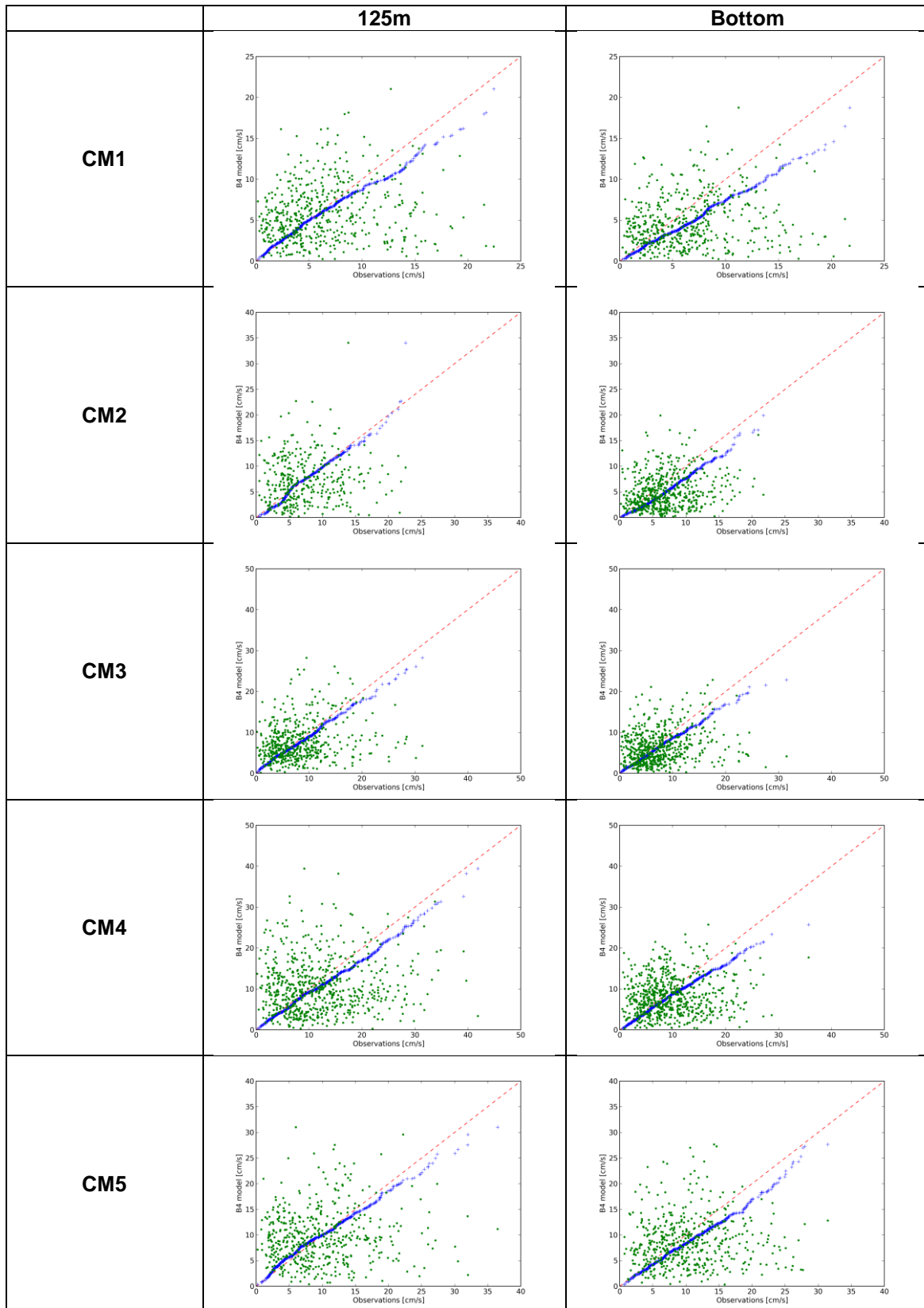


Figure 33: Combined qq- and scatterplots for current speed (in cm/s) over the years 2000 - 2001 in the Fugløya - Bjørnøya section at each station (CM1 - CM5). Observations are along the horizontal axis and BaSIC4 model along the vertical axis. The left column shows results at 125m depth, and the right column shows results for the bottom depths. Green dots are the scatterplots, and blue “plus-signs” indicate the qq-plots.

### 3.2.2 Temperature and salinity

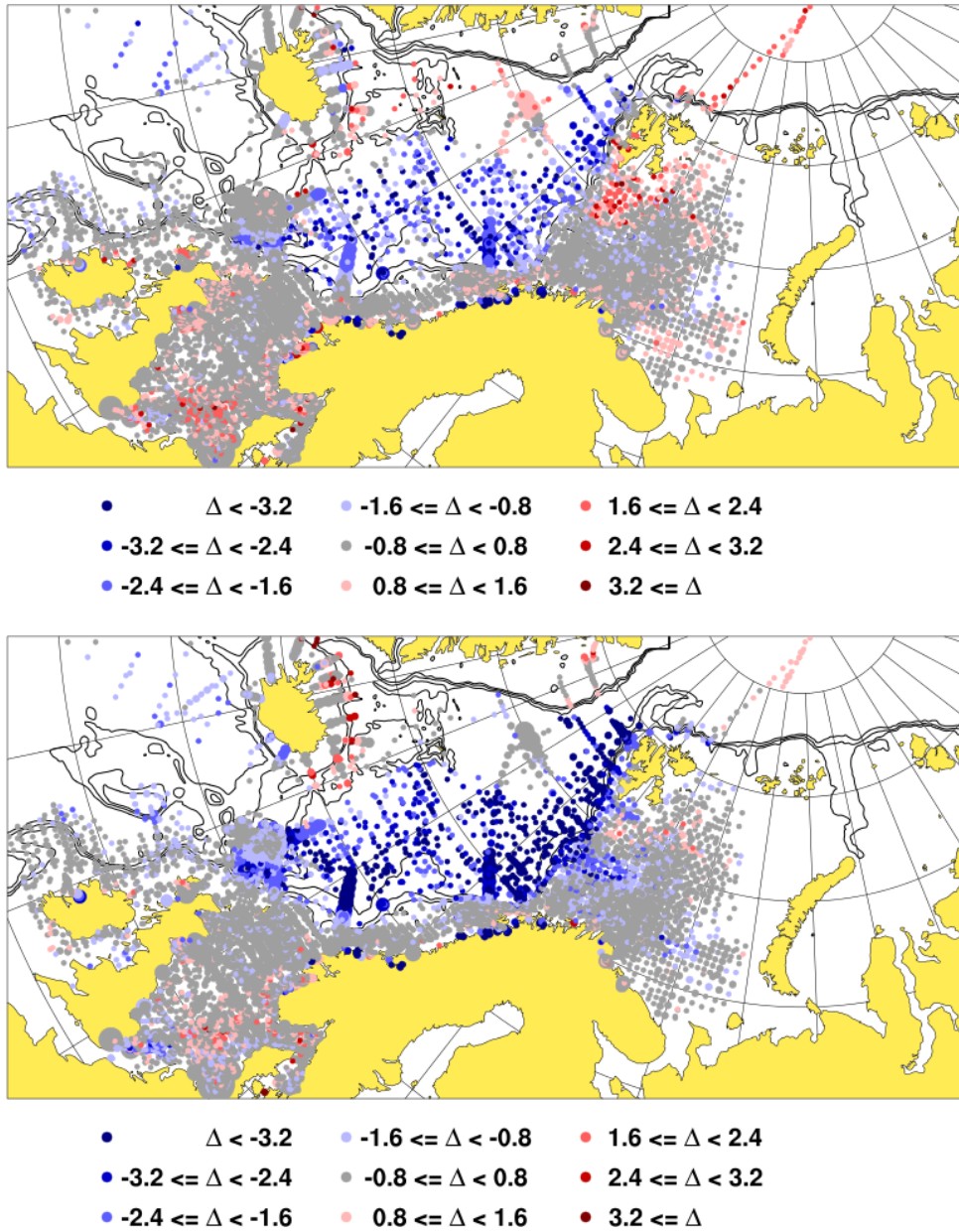


Figure 34: Maps displaying the distribution of temperature observations, with a colour code that represents the model vs. observation differences. The relation between differences and each colour coded range is displayed at the bottom of the figures. Results from BaSIC4 and SVIM4 are shown in the top and bottom panels, respectively.

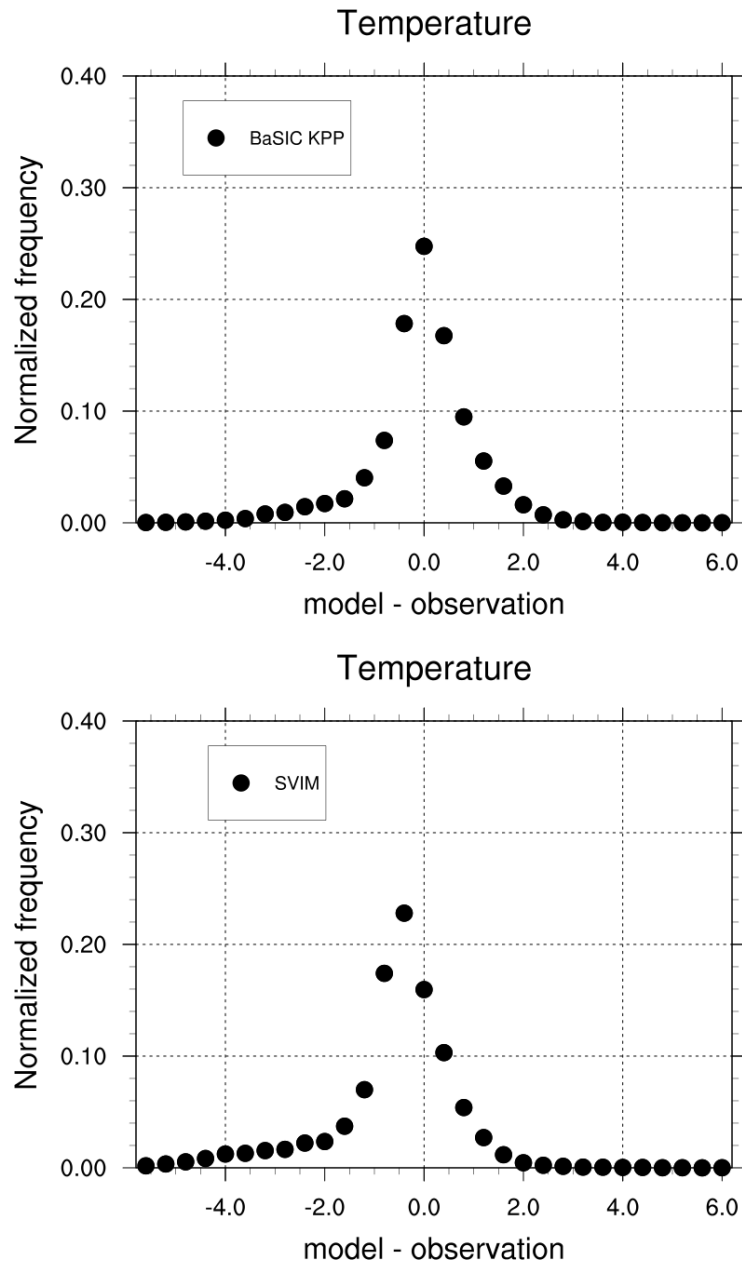


Figure 35: Probability distributions of differences in potential temperature (averages over top 100m). Values were aggregated in bins of 0.4K, and the amplitude is normalized by dividing the number of entries in each bin by the total no. of observations. The bias and standard deviation in BaSIC4 (top panel) were -0.05K and 1.05K, respectively. The corresponding values in SVIM4 (bottom panel) were -0.61K and 1.27K. Data from 11,005 profiles were included.

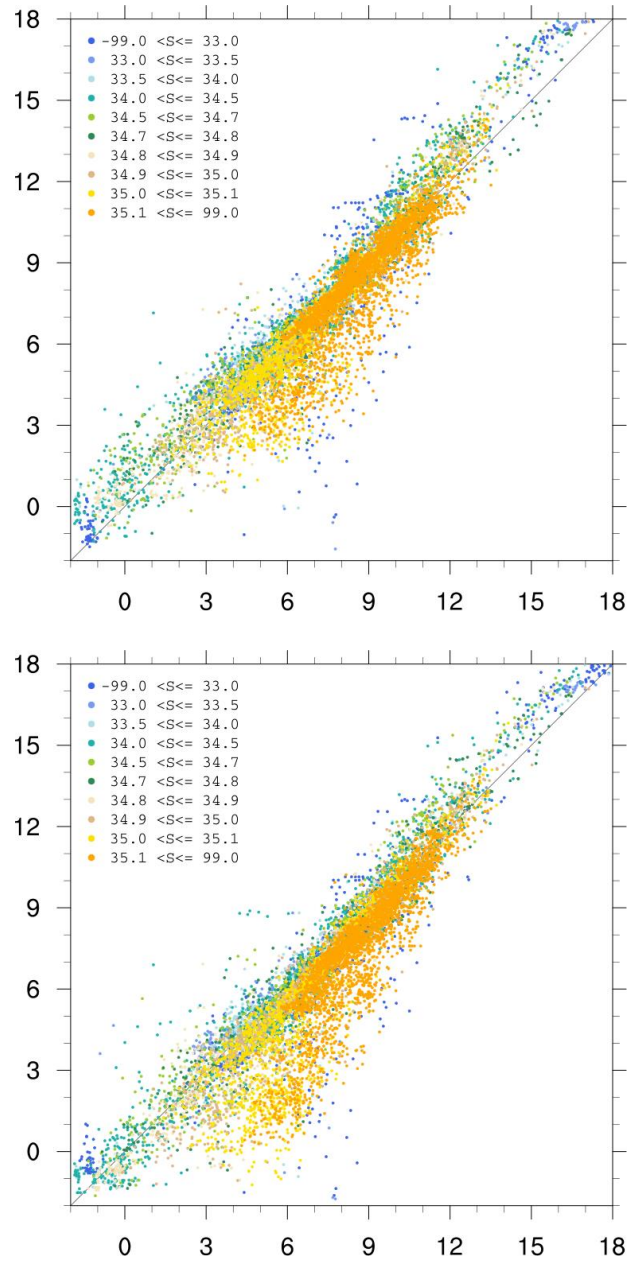


Figure 36: Scatter plots for averaged potential temperature from the upper 100m of the water column, for observations (horizontal axis) vs. model results (vertical axis). The colour code corresponds to the corresponding salinity average in the observations. High salinity dots are plotted on top. Results from BaSIC4 and SVIM4 are shown in the top and bottom panels, respectively.

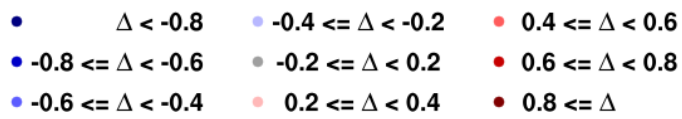
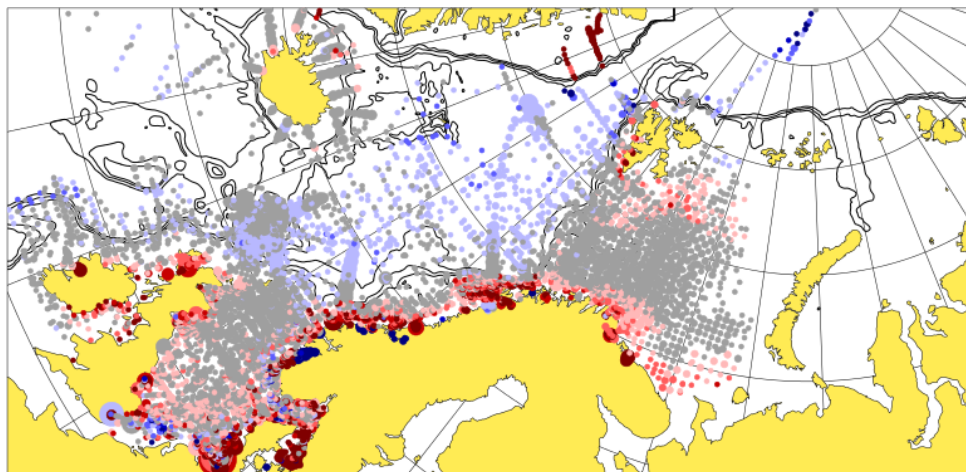
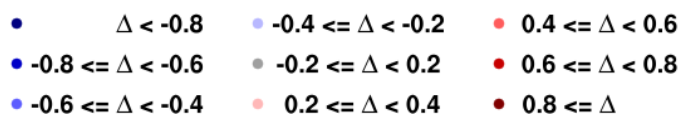
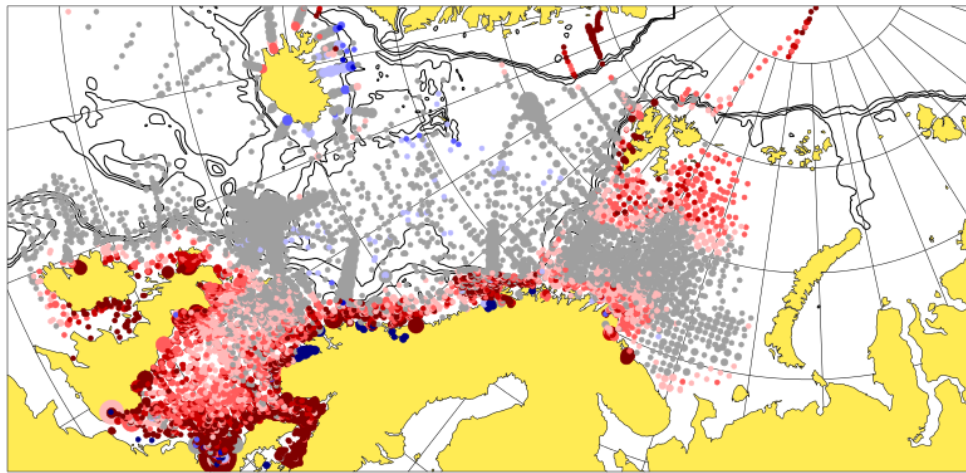


Figure 37: Same as Figure 34, but for salinity offset. BaSIC4 in top panel and SVIM4 in bottom panel.

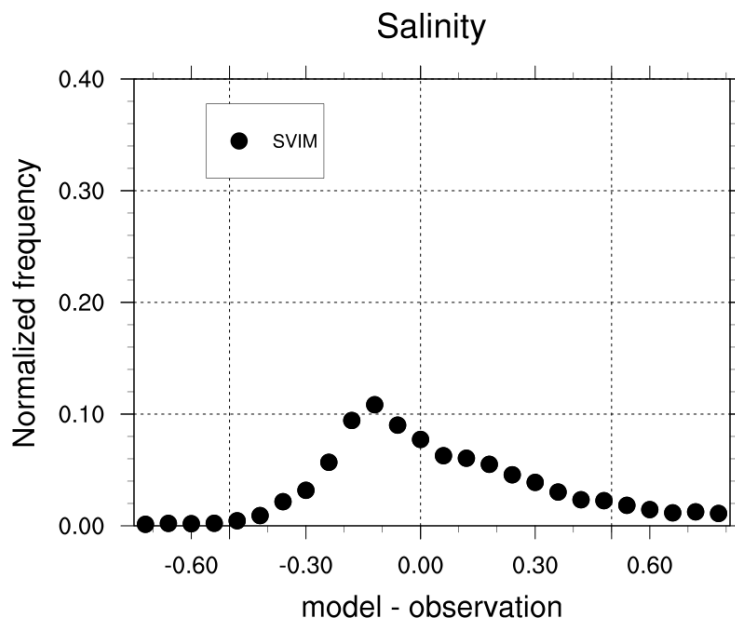
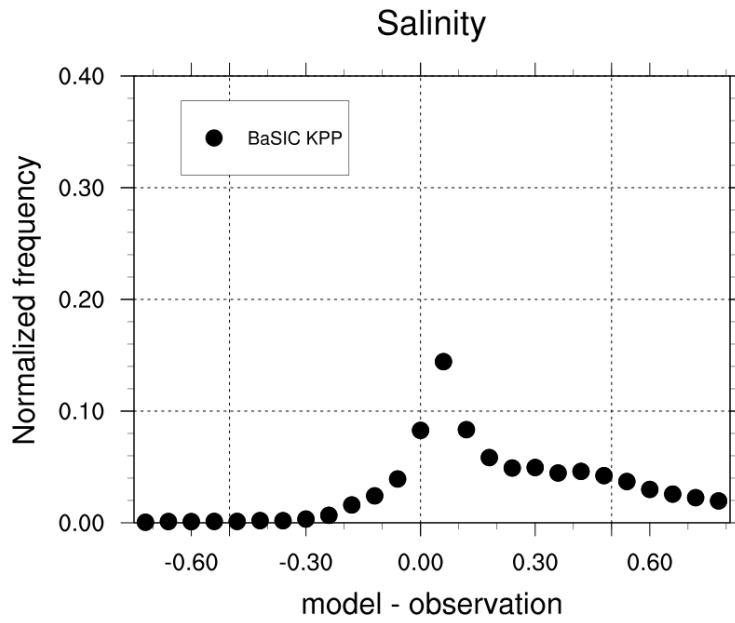


Figure 38: Same as Figure 35, but for salinity. Values were aggregated in bins of 0.06ppt. The bias and standard deviation in BaSIC4 were +0.339ppt and 1.202ppt, respectively. The corresponding values in SVIM4 were +0.114ppt and 1.018ppt.

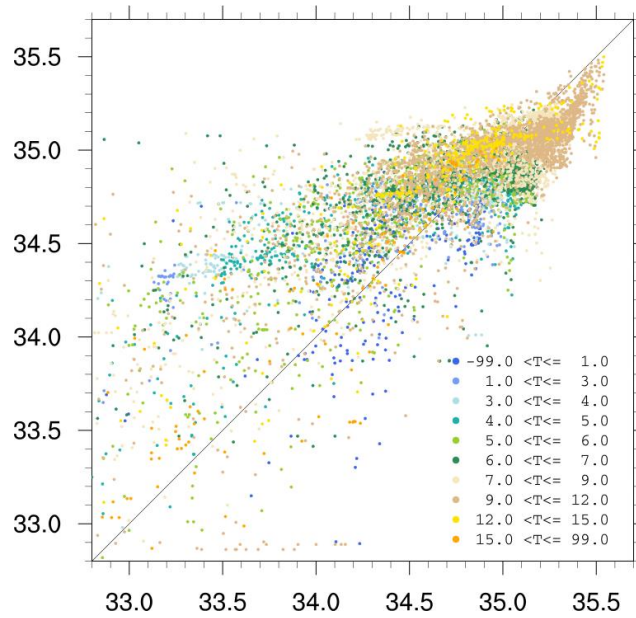
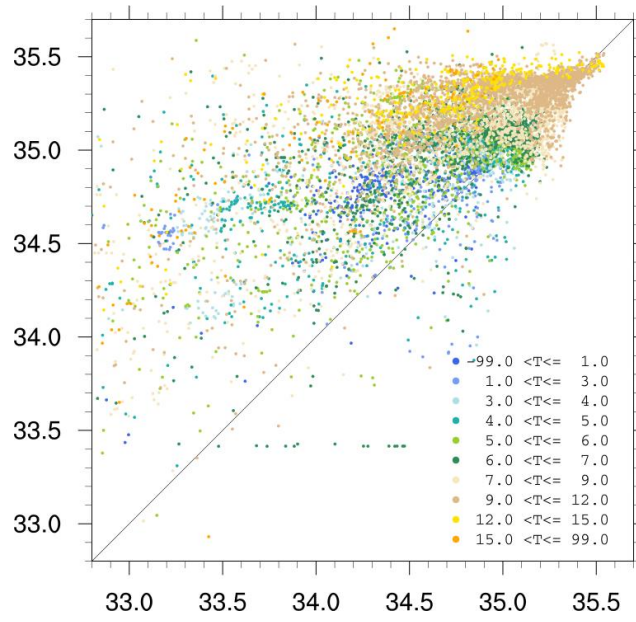


Figure 39: Same as Figure 36, but for salinity. The colour code corresponds to observed temperature, with warm dots plotted on top.

### 3.2.3 Sea ice

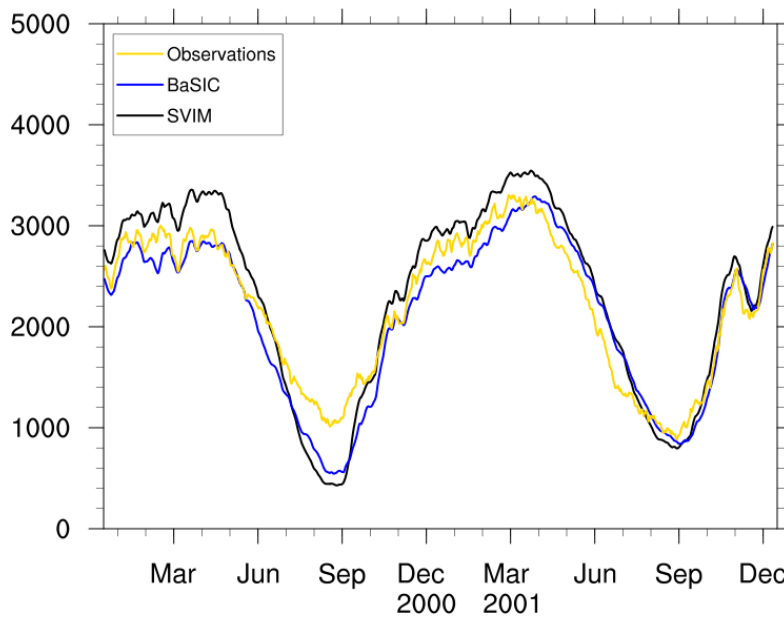


Figure 40: Time series of sea ice area (integral of sea ice concentration) in the domain of the BaSIC4 and SVIM4 model configurations. OSI SAF observations are displayed by the yellow line, while model results from BaSIC4 and SVIM4 are shown by the blue and black lines, respectively. Overall averages are (in  $Mkm^2$ ) 2.21 (OSI SAF), 2.11 (BaSIC4), and 2.32 (SVIM4).

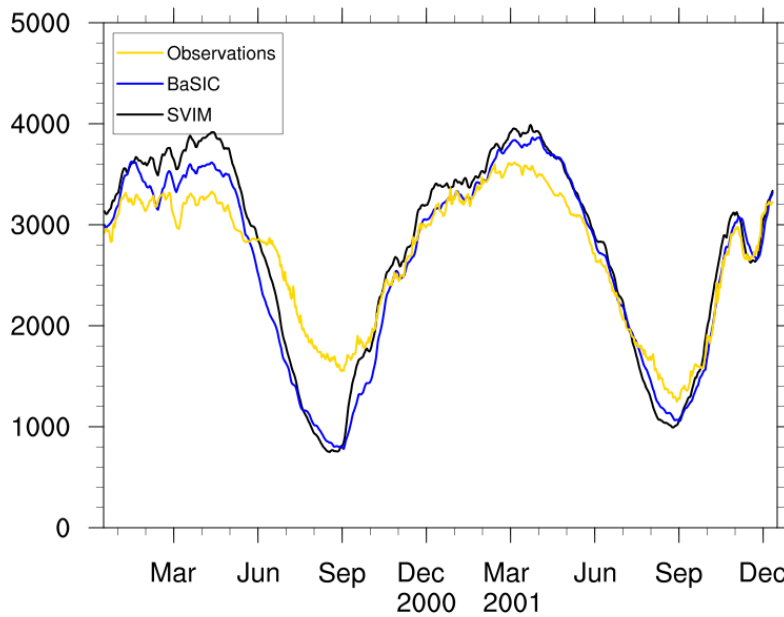


Figure 41: Same as Figure 40, but for time series of sea ice extent (area where the sea ice concentration exceeds 0.15). Overall averages are (in  $Mkm^2$ ) 2.68 (OSI SAF), 2.63 (BaSIC4), and 2.75 (SVIM4).

## 4 Comparison of current speed for different model resolution

The main objective of this chapter is to compare how the horizontal resolution of the model domain affects the predicted current speed. This will in turn help us to decide on the resolution of the final BaSIC-model.

For each of the stations, CM1 through CM5, we have looked at the top and bottom layer of the model. The comparison is done as qq-plots. It has the highest resolution model along the horizontal axis and the lowest resolution model along the vertical axis. In each of the figures there are both red dots and blue stars. For the blue stars we simply pick the closest gridpoint to the station in each of the two models. For the red dots we pick the closest gridpoint to the station in the low resolution model and from the high resolution model we average gridpoints surrounding the station so that the high resolution model is averaged to the same resolution as the low resolution model.

As expected these comparisons show that the highest current speeds are found in the highest resolution models.

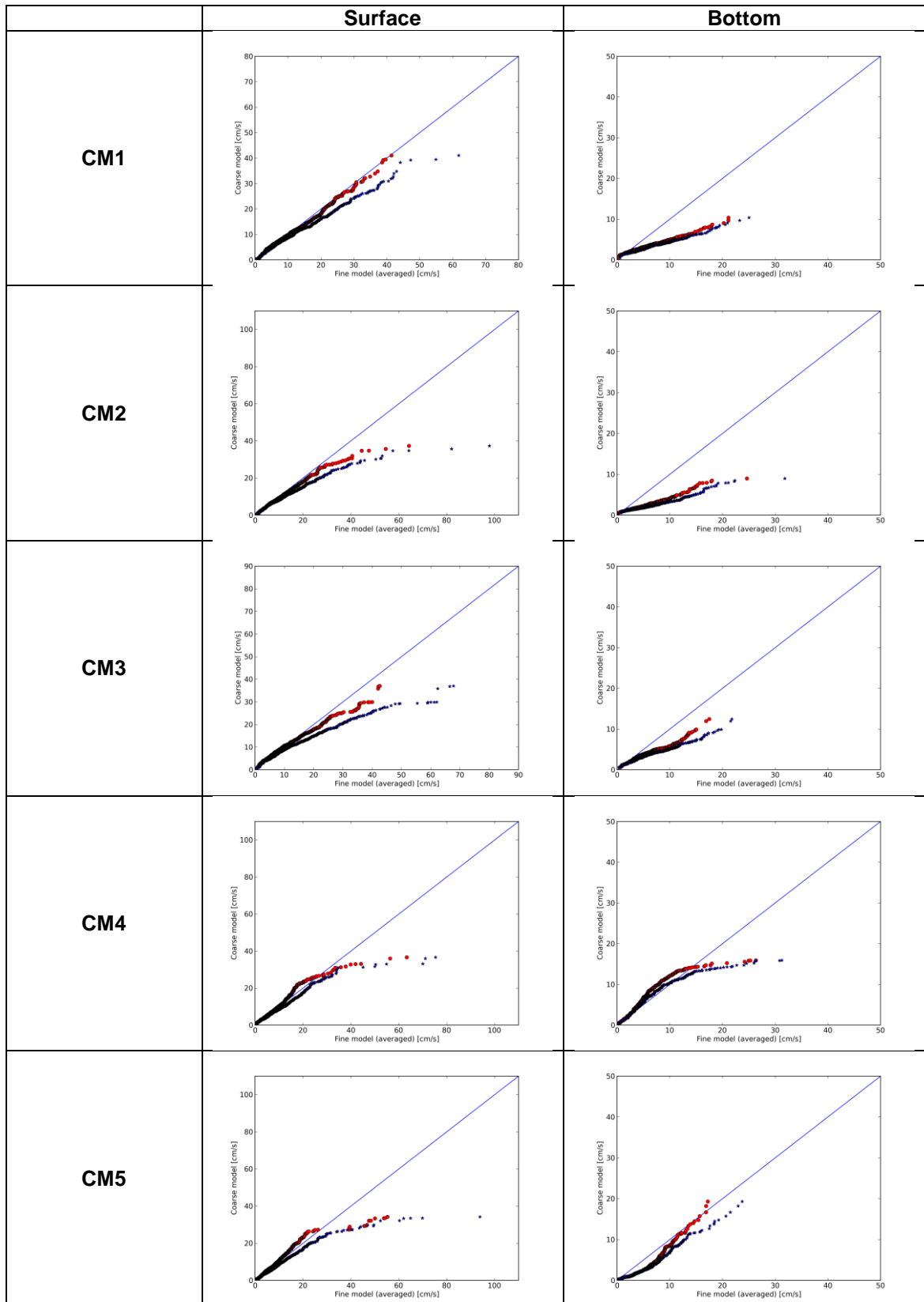


Figure 42: Comparison of current speed form BaSIC20 and BaSIC2 models. For detailed explanations, see page 48.

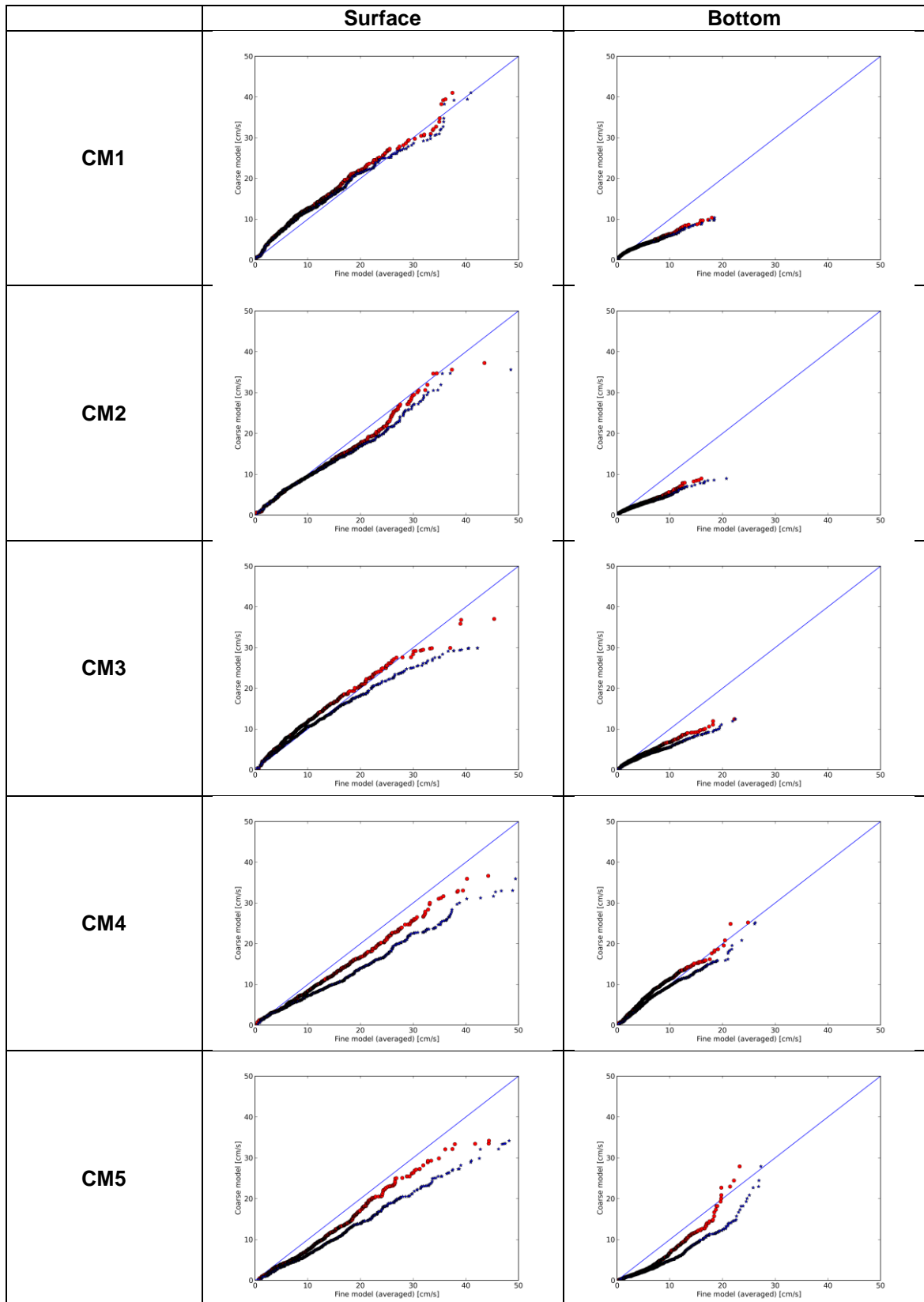


Figure 43: Comparison of current speed form BaSIC20 and BaSIC4 models. For detailed explanations, see page 48.

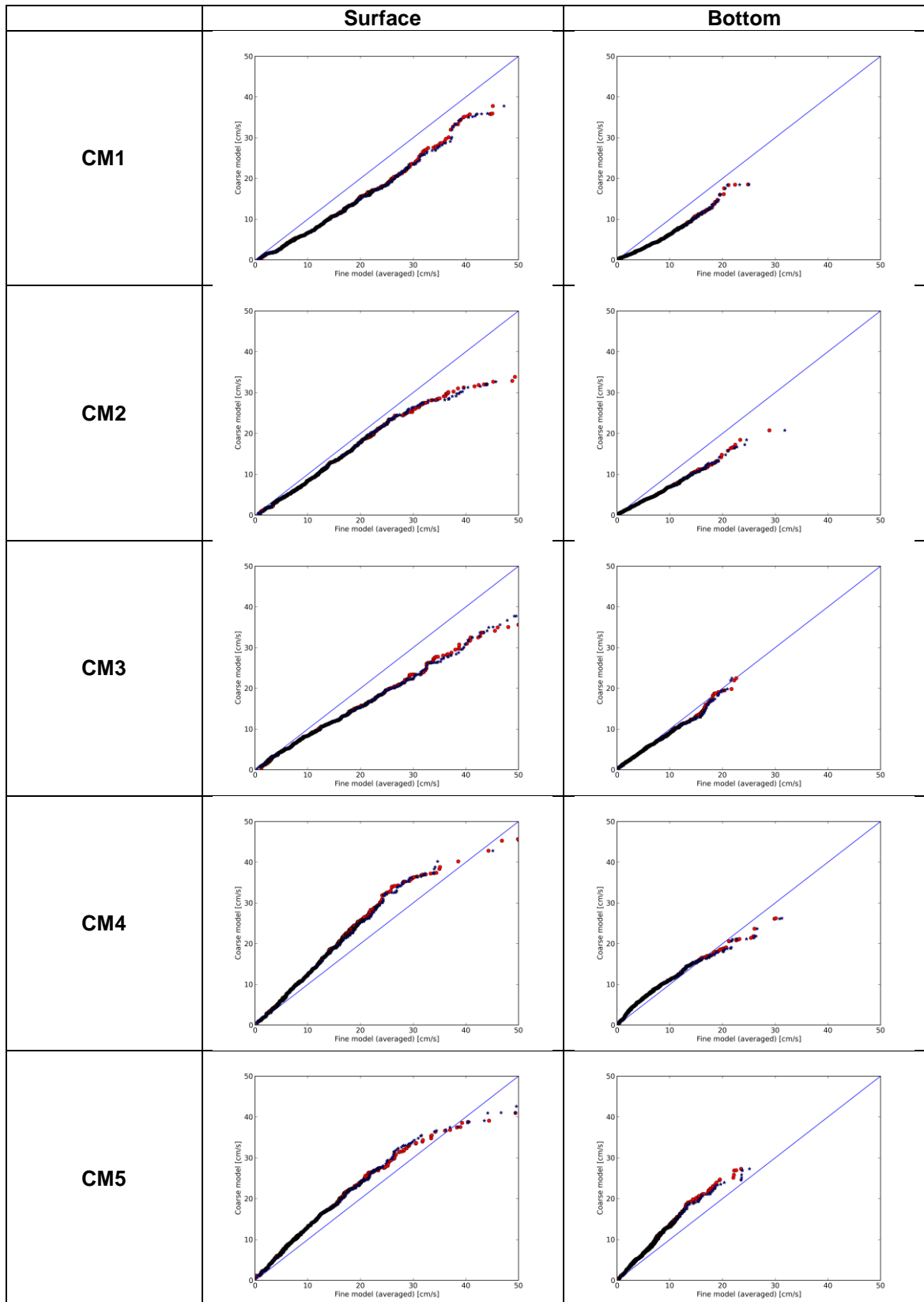


Figure 44: Comparison of current speed form BaSIC4 and BaSIC2 models. For detailed explanations, see page 48.



## 5 Conclusions and recommendations

After the discrepancies that were revealed by the validation of the previous trial hindcast in the BaSIC-project (as described in MET report no. 12/2013), we decided, in agreement with Statoil, to perform further tests and a new trial hindcast.

### 5.1 Conclusions

Based on the comparison of the previous hindcast, as documented in MET report no. 12/2013, and the present one, we conclude that the new setup provides better and more realistic statistics of current speeds in the Barents Sea opening (Fugløya – Bjørnøya cross section). The new setup also has lower bias and standard deviation for temperature than SVIM4, but there is an issue with salinity. In this regard we note that SVIM4 was run with relaxation of surface salinity towards climatology, and we recommend introducing similar techniques in BaSIC. For sea-ice, the results in the present setup are of comparable or better quality than those in the previous setup.

The main focus in this new hindcast was to improve the statistics of the current hindcast. When comparing qq-plots and PDFs from this report and MET report 12/2013, one clearly sees that the new setup outperforms all the previous models with regards to both speed and direction. Regarding the question of resolution the above results show that a 4 km mesh size may suffice. We recommend testing this in the continuation of BaSIC, and if necessary running a limited area model with a higher resolution.

### 5.2 Recommendations

We recommend continuing the BaSIC project. The new model setup is very promising, and we expect it to produce a hindcast that fulfils Statoil's requirements.

However, for the production we suggest the following modifications to be considered:

- Introduce correction/relaxation of salinity towards climatology.
- Look at the possibilities of nesting the model to a model covering the Baltic Sea, or other actions to improve salinity in Skagerrak, and hence in the Norwegian Coastal Current.

- The hindcast should start at around 1980. This is 13 years before the FOAM reanalysis starts. We suggest making a climatology based on the FOAM reanalysis for this period and if needed we can perturb this climatology with interannual variability based on SODA or similar.

## Acknowledgements

This work is funded by Statoil through Contract No. 4502465983.

## References

Andersen, S., L.-A. Breivik, S. Eastwood, et al. (2012), OSI SAF Sea Ice Product Manual, Tech. rep. SAF/OSI/met.no/TEC/MA/125, EUMETSAT OSI SAF - Ocean and Sea Ice Satellite Application Facility.

Boyer, T.P., J.I. Antonov, O.K. Baranova, H.E. Garcia, D.R. Johnson, R.A. Locarnini, A.V. Mishonov, T.D. O'Brien, D. Seidov, I. V. Smolyar, and M.M. Zweng (2009), World Ocean Database, NOAA Atlas NESDIS 66 - U.S. Gov. Print. Off., Wash. D.C. 216pp., DVDs.

Eastwood, S., K.R. Larsen, T. Lavergne, E. Nielsen, and R. Tonboe (2011), OSI SAF Global Sea Ice Concentration Reprocessing, User Manual, Tech. Rep. SAF/OSI/met.no/TEC/MA/138, EUMETSAT OSI SAF - Ocean and Sea Ice Satellite Application Facility.

